Deutsche Forschungsgemeinschaft

Priority Programme 1962

First and Second Order Shape Optimization Based on Restricted Mesh Deformations

Tommy Etling, Roland Herzog, Estefanía Loayza, Gerd Wachsmuth

SPP 1962

Non-smooth and Complementarity-based Distributed Parameter Systems: Simulation and Hierarchical Optimization

Preprint Number SPP1962-088

received on October 24, 2018

Edited by
SPP1962 at Weierstrass Institute for Applied Analysis and Stochastics (WIAS)
Leibniz Institute in the Forschungsverbund Berlin e.V.
Mohrenstraße 39, 10117 Berlin, Germany
E-Mail: spp1962@wias-berlin.de

World Wide Web: http://spp1962.wias-berlin.de/

FIRST AND SECOND ORDER SHAPE OPTIMIZATION BASED ON RESTRICTED MESH DEFORMATIONS*

TOMMY ETLING†, ROLAND HERZOG†, ESTEFANÍA LOAYZA†, AND GERD WACHSMUTH‡

Abstract. We consider shape optimization problems subject to elliptic partial differential equations. In the context of the finite element method, the geometry to be optimized is represented by the computational mesh, and the optimization proceeds by repeatedly updating the mesh node positions. It is well known that such a procedure eventually may lead to a deterioration of mesh quality, or even an invalidation of the mesh, when interior nodes penetrate neighboring cells. We examine this phenomenon, which can be traced back to the ineptness of the discretized objective when considered over the space of mesh node positions. As a remedy, we propose a restriction in the admissible mesh deformations, inspired by the Hadamard structure theorem. First and second order methods are considered in this setting. Numerical results show that mesh degeneracy can be overcome, avoiding the need for remeshing or other strategies.

Key words. shape optimization, shape gradient, gradient descent

AMS subject classifications. 90C30, 90C46, 65K05

1. Introduction. Shape optimization is ubiquitous in the design of structures of all kinds, going from drug eluting stents Zunino, 2004 until aircraft wings Schmidt, Gauger, et al., 2011 or horn-like structures appearing in devices for acoustic or electromagnetic waves Udawalpola, Berggren, 2008. All of these and many other applications involve the solution u of a partial differential equation (PDE), so the general formulation of shape optimization problems considered here is as follows:

$$\min_{\Omega} J(\Omega, u(\Omega)). \tag{1.1}$$

Here $u(\Omega)$ is the solution of the underlying PDE defined on the domain Ω, which is to be optimized.

Computational approaches to solving PDE-constrained shape optimization problems usually proceed along the following lines. First, one derives an expression for the *Eulerian derivative* of the objective w.r.t. vector fields which describe the perturbation of the current domain Ω. The perturbations are carried out either in terms of the perturbation of identity, or the velocity method. The Eulerian derivative can be

*Submitted to the editors October 24, 2018.

Funding: This work was partially supported by DFG grants HE 6077/10–1 and WA 3636/4–1 within the Priority Program SPP 1962, which is gratefully acknowledged.

†Technische Universität Chemnitz, Faculty of Mathematics, Professorship Numerical Mathematics (Partial Differential Equations), 09107 Chemnitz, Germany (TE: tommy.etling.tu-chemnitz.de, https://www.tu-chemnitz.de/mathematik/part_dgl/people/etling; RH: roland.herzog@mathematik.tu-chemnitz.de, https://www.tu-chemnitz.de/herzog; EL: estefania.loayza@mathematik.tu-chemnitz.de, https://www.tu-chemnitz.de/mathematik/part_dgl/people/loayza).

‡Brandenburgische Technische Universität Cottbus-Senftenberg, Institute of Mathematics, Chair of Optimal Control, Platz der Deutschen Einheit 1, 03046 Cottbus, Germany (gerd.wachsmuth@b-tu.de, https://www.b-tu.de/fg-optimale-steuerung).

stated either as an expression concentrated on the boundary $\partial\Omega$, or as a volume expression. The first is due to the Hadamard structure theorem (Sokołowski, Zolésio, 1992, Theorem 2.27). For volume expressions, we refer the reader, for instance, to Laurain, Sturm, 2016; Hiptmair, Paganini, Sargheini, 2015. Second, the Eulerian derivative, which represents a linear functional on the perturbation vector fields, needs to be converted into a vector field V itself, often referred to as the *shape gradient*. This can be achieved by evaluating the Riesz representative of the derivative w.r.t. an inner product. The latter is often chosen as the bilinear form associated with the Laplace-Beltrami operator on $\partial\Omega$, or with the linear elasticity (Lamé) system on Ω, see e.g. Schmidt, Gauger, et al., 2011; Schulz, Siebenborn, 2016; Schmidt, Schulz, 2010; 2009. More sophisticated techniques include quasi-Newton or Hessian-based inner products; see Eppler, Harbrecht, 2005; Novruzi, Roche, 2000; Schulz, Siebenborn, Welker, 2015; Schulz, 2014. This perturbation field is then used to update the domain Ω inside a line search method, where the transformed domain

$$\Omega_t = \{x + t\,V(x) : x \in \Omega\} \tag{1.2}$$

associated with the step size t is obtained from the perturbation of identity approach.

While the computation of the Eulerian derivative is either based on the continuous or some discrete formulation of problem (1.1), the computation of the shape gradient and the subsequent updating steps will always be carried out in the discrete setting. Typically, the shape Ω is represented by a computational mesh, and the underlying PDE is solved, e.g., by the finite element method. The perturbation field V is then expressed as a piecewise linear field, i.e., it is represented in terms of a velocity vector attached to each vertex position. The domain Ω is subsequently updated according to (1.2) inside a line search procedure.

It has been observed in many publications that this straightforward approach has one major drawback: it often leads to a degeneracy of the computational mesh. This degeneracy manifests itself in different ways, but mostly through degrading cell aspect ratios, or even mesh nodes entering neighboring cells. Indeed, Doğan et al., 2007 observe that

> It is typical of surface evolution undergoing large deformations that triangles may tangle and cross, and that their angles may become large. These mesh distortions limit resolution and approximability, as well as impair computations, thereby leading to numerical artifacts.

In practice, both phenomena often lead to a breakdown of computational shape optimization procedures.

Over the past 10 years, a range of various techniques have been proposed to circumvent this major obstacle in computational shape optimization. A natural choice is to remesh the computational domain; see for instance Wilke, Kok, Groenwold, 2005; Morin et al., 2012; Sturm, 2016; Dokken et al., 2018; Feppon et al., 2018. In fact, Morin et al., 2012 point out that

> A rule of thumb for dealing with complicated domain deformations is that remeshing is indispensable and unavoidable.

Remeshing can be carried out either in every iteration or whenever some measure of mesh quality falls below a certain threshold. Drawbacks of remeshing include the high computational cost and the discontinuity introduced into the history of the objective values.

Bänsch, Morin, Nochetto, 2005; Doğan et al., 2007 describe several techniques such as mesh regularization, space adaptivity, angle control in addition to a semi-implicit Euler discretization for the velocity method, with time adaptivity and backtracking line search. In a follow-up work, Morin et al., 2012 consider a line-search method that aims to avoid mesh distortion due to tangential movements of the boundary nodes, combined with a geometrically consistent mesh modification (GCMM) proposed in Bonito, Nochetto, Pauletti, 2010. Giacomini, Pantz, Trabelsi, 2017 address the issue of spurious descent directions, attributed to discretization errors in the underlying PDE model, via a goal-oriented mesh adaptation approach. Recently, Iglesias, Sturm, Wechsung, 2017 proposed to enforce shape gradients from nearly conformal transformations, which are known to preserve angles and ensure a good quality of the mesh along the optimization process.

Finally, we mention Schulz, Siebenborn, Welker, 2015; 2016; Schulz, Siebenborn, 2016, who advocate the linear elasticity model as the inner product to convert Eulerian derivative into a shape gradient. In particular in Schulz, Siebenborn, Welker, 2016 the authors propose to omit the assembly of interior contributions appearing in the discrete volume expression of the Eulerian derivative. This approach is vaguely related to but conceptionally different from our idea and no analysis is provided there.

Our Contribution. In this paper we propose an approach to avoid spurious descent directions in the course of numerical shape optimization procedures, which is different from all of the above. The main idea is based on the observation that—in the continuous setting—shape gradients are perturbation fields which are generated exclusively by normal forces on the boundary of the current domain. This follows from the Hadamard structure theorem. However, in the discrete setting, the Hadamard structure theorem is not available, and thus classical discrete shape gradients also contain contributions from interior forces and tangential boundary forces. We therefore propose to project the shape gradient onto the subspace of perturbation fields generated by normal forces. We refer to this approach as *restricted mesh deformations*.

We demonstrate that the proposed approach indeed avoids spurious descent directions and degenerate meshes. As a consequence, we can solve discrete shape optimization problems to high accuracy, i.e., very small norm of the restricted gradient. Both gradient and Newton schemes are considered.

The paper is structured as follows. In section 2 we present a shape optimization model problem and prove, as an auxiliary result, the existence of a globally optimal domain. In section 3 we review the volume and boundary representations of the Eulerian derivative. In section 4 we consider the discrete counterpart of the model problem and its Eulerian derivative. We also illustrate the detrimental effect of spurious descent directions. The main idea of restricted mesh deformations is introduced in section 5. An associated *restricted gradient scheme* is also introduced and its performance is compared to the classical shape gradient method in section 6. Sections 7 and 8 are devoted to second-order Eulerian derivatives in the restricted setting and the demonstration of the associated Newton scheme. Finally we present in section 9 a new result on the convergence of a sequence of stationary domains for discrete shape optimization problems to a stationary point of the continuous problem as the discretization mesh size goes to zero. Conclusions are given in section 10.

2. Preliminaries. Throughout the paper, we consider the following model problem,

$$\text{Minimize} \quad \int_\Omega u \, \mathrm{d}x \quad \text{s.t.} \quad \Omega \subset D \text{ is open}, \begin{cases} -\Delta u = f & \text{in } \Omega, \\ \quad u = 0 & \text{on } \partial\Omega. \end{cases} \tag{2.1}$$

Here the optimization variable $\Omega \subset \mathbb{R}^d$ is an admissible domain contained in some bounded and open hold-all $D \subset \mathbb{R}^d$, and $f \in H^1(D)$ is a given right hand side. The elliptic state equation is understood in weak form,

$$\text{Find } u \in H_0^1(\Omega) \qquad \text{such that} \qquad \int_\Omega \nabla u \cdot \nabla v \, \mathrm{d}x = \int_\Omega f \, v \, \mathrm{d}x \quad \forall v \in H_0^1(\Omega). \tag{2.2}$$

The next result shows that our shape optimization problem (2.1) has a solution if we slightly relax the class of admissible sets. We will see that it is sufficient to consider *quasi-open* rather than open sets. For an introduction of quasi-open sets, quasi-continuity and related notions, we refer the reader to Attouch, Buttazzo, Michaille, 2014, Section 5.8. We consider the slightly relaxed problem

$$\text{Minimize} \quad \int_\Omega u \, \mathrm{d}x \quad \text{s.t.} \quad \Omega \subset D \text{ is quasi-open}, -\Delta u = f \text{ in } H^{-1}(\Omega). \tag{2.3}$$

Let us recall that $H_0^1(\Omega) = \{u \in H_0^1(\mathbb{R}^d) \mid u = 0 \text{ q.e. in } \mathbb{R}^d \setminus \Omega\}$ and $H^{-1}(\Omega)$ is the dual space of $H_0^1(\Omega)$. The PDE in (2.3) is also to be understood in the weak sense, i.e.,

$$\text{Find } u \in H_0^1(\Omega) \qquad \text{such that} \qquad \int_D \nabla u \cdot \nabla v = \int_D f \, v \, \mathrm{d}x \quad \forall v \in H_0^1(\Omega).$$

We emphasize that the main reason for this existence result is that the objective is monotone w.r.t. the state u, see also Remark 2.3 below.

THEOREM 2.1. *Problem (2.3) admits a global minimizer $(\hat\Omega, \hat u)$.*

Note that the extreme case $(\hat\Omega, \hat u) = (\emptyset, 0)$ is possible.

Proof. First, we remark that it is sufficient to consider only pairs $(\{u < 0\}, u)$ with $u \le 0$ in (2.3). Indeed, if (Ω, u) is any admissible pair, we can consider $(\{u < 0\}, \min(u, 0))$ in its stead. Note that $\{u < 0\}$ is quasi-open since u can chosen to be quasi-continuous. This pair is again admissible due to

$$\int_D \nabla \min(u, 0) \cdot \nabla v \, \mathrm{d}x = \int_\Omega \nabla u \cdot \nabla v \, \mathrm{d}x = \int_D f \, v \, \mathrm{d}x \qquad \forall v \in H_0^1(\{u < 0\}),$$

since $v = 0$ q.e. on $\Omega \setminus \{u < 0\}$. Moreover, the objective value of $(\{u < 0\}, \min(u, 0))$ is not larger than the objective value of (Ω, u).

Now, let $\{(\Omega_n, u_n)\}$ be a minimizing sequence for (2.3) with $u_n \le 0$ and $\Omega_n = \{u_n < 0\}$. It is clear that the sequence $\{u_n\}$ is bounded in $H_0^1(D)$, therefore we can extract a weakly convergent subsequence (without relabeling) with weak limit u.

Clearly, $u \le 0$. Now we define $\hat\Omega = \{u < 0\}$ and denote by $\hat u \in H_0^1(\hat\Omega)$ the solution of $-\Delta \hat u = f$ in $H^{-1}(\hat\Omega)$. It remains to check that $\hat u \le u$ holds since this implies the global optimality of $\hat u$ (due to the monotonicity of the objective). To this end, we choose an arbitrary $v \in H_0^1(D)$ such that $-u \ge v \ge 0$. For $v_n := \min(-u_n, v)$ we have $v_n \in H_0^1(\Omega_n)$ due to $v \ge 0$. Moreover, $v_n \rightharpoonup \min(-u, v) = v$ in $H_0^1(D)$, see Wachsmuth, 2016, Lemma 4.1. Thus,

$$\begin{aligned}\int_D f\, v \,\mathrm{d}x = \lim_{n\to\infty} \int_D f\, v_n \,\mathrm{d}x &= \lim_{n\to\infty} \int_D \nabla u_n \cdot \nabla v_n \,\mathrm{d}x \\ &= \lim_{n\to\infty} \int_D \nabla(u_n + v)\cdot\nabla(v_n - v) + \nabla u_n \cdot \nabla v - \nabla v \cdot \nabla(v_n - v)\,\mathrm{d}x \\ &= \lim_{n\to\infty} \int_D -\nabla|\min(-u_n - v, 0)|^2 + \nabla u_n \cdot \nabla v \,\mathrm{d}x \le \int_D \nabla u \cdot \nabla v \,\mathrm{d}x.\end{aligned}$$

Since $v \in H_0^1(\hat\Omega)$, we can test the equation for $\hat u$ with v and we find

$$\int_{\hat\Omega} \nabla(\hat u - u)\cdot\nabla v \,\mathrm{d}x \le 0 \qquad \forall v \in H_0^1(D) \text{ satisfying } -u \ge v \ge 0.$$

Now, we can use a density argument, see Mignot, 1976, Lemme 3.4, to obtain that this inequality holds for all $v \in H_0^1(\hat\Omega)$ which satisfy $v \ge 0$. Using $v = \max(\hat u - u, 0)$ implies $\max(\hat u - u, 0) = 0$, i.e., $\hat u \le u$. Finally, the optimality of $(\hat\Omega, \hat u)$ follows from

$$\int_D \hat u \,\mathrm{d}x \le \int_D u \,\mathrm{d}x = \lim_{n\to\infty} \int_D u_n \,\mathrm{d}x.$$

∎

Remark 2.2. There is a deeper reason for $\hat u \le u$ being true in the above proof. Indeed, using the theory of relaxed Dirichlet problems, one can show that u satisfies $-\Delta u + \mu\, u = f$ for some capacitary measure μ. We refer to Attouch, Buttazzo, Michaille, 2014, Section 5.8.4 for a nice introduction to capacitary measures. Due to $u \le 0$ we have (in a certain sense) $\mu\, u \le 0$ and therefore $\hat u \le u$ follows from the maximum principle since "$-\Delta \hat u = f \le f - \mu\, u = -\Delta u$". However, we included the above direct proof because it does not rely on the notion of capacitary measures.

Remark 2.3. The above proof of existence generalizes to a larger class of objective functionals. In fact, we can replace the objective in (2.3) with

$$\int_\Omega j(x, u(x)) \,\mathrm{d}x$$

if the integrand j satisfies

$$j(x, \cdot) \text{ is monotonically increasing on } (-\infty, 0] \text{ and non-negative on } [0, \infty), \tag{2.4a}$$

$$j(\cdot, u) \in L^1(D) \quad \forall u \in H_0^1(D), \tag{2.4b}$$

$$u_n \rightharpoonup u \text{ in } H_0^1(D) \text{ implies } \int_D j(u)\,\mathrm{d}x \le \liminf_{n\to\infty} \int_D j(u_n)\,\mathrm{d}x. \tag{2.4c}$$

Under these general assumptions, one can use the same proof as the one given for

Theorem 2.1 above, but the final estimate has to be replaced by

$$\begin{aligned}\int_{\hat\Omega} j(\cdot,\hat u)\,\mathrm{d}x \le \int_{\hat\Omega} j(\cdot,u)\,\mathrm{d}x &= \int_D j(\cdot,u) - j(\cdot,0)\,\mathrm{d}x + \int_{\{u<0\}} j(0)\,\mathrm{d}x \\ &\le \liminf_{n\to\infty} \int_D j(\cdot,u_n) - j(\cdot,0)\,\mathrm{d}x + \int_{\{u_n<0\}} j(0)\,\mathrm{d}x \\ &= \liminf_{n\to\infty} \int_{\Omega_n} j(\cdot,u_n)\,\mathrm{d}x.\end{aligned}$$

Note that Fatou's lemma together with $u_n \to u$ a.e. (along a subsequence) implies

$$\int_{\{u<0\}} j(0)\,\mathrm{d}x \le \liminf_{n\to\infty} \int_{\{u_n<0\}} j(0)\,\mathrm{d}x.$$

Again, this shows the optimality of $(\hat\Omega,\hat u)$.

3. Shape Calculus. This section is devoted to the presentation of the shape differentiability of problem (2.1). Since this is rather standard problem we will be able to directly apply results from Ito, Kunisch, Peichl, 2008. To this end, we assume that both the hold-all $D \subset \mathbb{R}^d$ and $\Omega \subset \mathbb{R}^d$ are open and have $C^{1,1}$-boundaries ∂D and $\partial\Omega$, respectively. Moreover we assume $\overline{\Omega} \subset D$ so that Ω has a positive distance to the boundary of D.

We are describing variations of the domain Ω by the *perturbation of identity method*, i.e., we consider a family of transformations $\{T_t\}_{t\in[0,\tau]}$ such that

$$T_t = \mathrm{id} + t\,V, \tag{3.1}$$

where $V \in C^{1,1}(D)^d$ is a given vector field. The family $\{T_t\}$ creates a family of perturbed domains $\Omega_t = T_t(\Omega)$. In view of Banach's fixed point theorem, there exists a bound $\tau > 0$ such that T_t is invertible for all $t \in [0,\tau]$.

By a straightforward application of Ito, Kunisch, Peichl, 2008, Theorem 2.1 we obtain the following result.

Theorem 3.1. *The shape functional given in* (2.1) *is shape differentiable and its Eulerian derivative in the direction of the perturbation field V is given by*

$$\begin{aligned}J'(\Omega;V) = \int_\Omega u\,(\operatorname{div} V)\,\mathrm{d}x \\ + \int_\Omega (\nabla u)^\top \left[(\operatorname{div} V)\,\mathrm{id} - DV - DV^\top\right] \nabla p\,\mathrm{d}x - \int_\Omega \operatorname{div}(f\,V)\,p\,\mathrm{d}x\end{aligned} \tag{3.2}$$

where DV denotes the Jacobian of V and the adjoint state p is the unique solution of the following adjoint problem,

$$\text{Find } p \in H_0^1(\Omega) \quad \text{such that} \quad \int_D \nabla p\cdot\nabla v\,\mathrm{d}x = -\int_D v\,\mathrm{d}x \quad \text{for all } v \in H_0^1(\Omega). \tag{3.3}$$

Notice that (3.2) is the so-called volume or weak formulation of the Eulerian derivative of (2.1). Besides the volume formulation, there exists an alternative representation of (3.2) by virtue of the well known Hadamard structure theorem; see Delfour, Zolésio, 2011, Chapter 9, Theorem 3.6. We state it here in a particularized version for problem (2.1). From now on, ν denotes the outer unit normal vector along the boundary $\partial\Omega$ of Ω.

COROLLARY 3.2 (Hadamard structure theorem for (2.1)). *The Eulerian derivative (3.2) of problem (2.1) has the representation*

$$J'(\Omega; V) = \int_{\partial\Omega} g_\Omega \, (V \cdot \nu) \, \mathrm{d}s \quad \textit{with } g_\Omega = -\frac{\partial u}{\partial \nu} \frac{\partial p}{\partial \nu}. \tag{3.4}$$

Notice that under the assumption that Ω has a $C^{1,1}$-boundary, u and p belong to $H^2(\Omega)$ and thus their normal derivatives are in $H^{1/2}(\partial\Omega)$, which embeds into $L^4(\partial\Omega)$ when $d \le 3$; see for instance Adams, Fournier, 2003, Theorem 4.12. Consequently, $g_\Omega = -\frac{\partial u}{\partial \nu} \frac{\partial p}{\partial \nu}$ belongs to $L^2(\partial\Omega)$ in this case.

Formula (3.4) is known as the boundary or strong representation of (3.2), and it can be obtained from (3.2) by the divergence theorem; compare Sturm, 2015, Sokołowski, Zolésio, 1992, Chapter 3.3, Haslinger, Mäkinen, 2003, Example 3.3. We also refer the reader to Hiptmair, Paganini, Sargheini, 2015, where the volume and boundary formulations are compared w.r.t. their order of convergence in a finite element setting.

4. Investigation of the Discrete Objective. In order to solve the shape optimization problem (2.1) numerically, some kind of discretization has to be applied. The most common choice in the literature consists in a discretization of the PDE by some finite element space defined over a computational mesh, which we denote by Ω_h and whose nodal positions serve to represent the discrete unknown domain.

A common choice is to replace $H^1_0(\Omega)$ by the finite element space of piecewise linear, globally continuous functions,

$$S^1_0(\Omega_h) = \{u \in H^1_0(\Omega_h) : u\big|_T \in \mathcal{P}_1(T) \text{ for all cells } T \text{ in } \Omega_h\} \tag{4.1}$$

defined over an approximation Ω_h of Ω consisting of geometrically conforming simplicial cells, i.e., triangles and tetrahedra in $d = 2$ or $d = 3$ space dimensions, respectively. Consequently, the state equation (2.2) is replaced by

$$\text{Find } u_h \in S^1_0(\Omega_h) \quad \text{such that} \quad \int_\Omega \nabla u_h \cdot \nabla v_h \, \mathrm{d}x = \int_\Omega f \, v_h \, \mathrm{d}x \quad \forall v_h \in S^1_0(\Omega_h). \tag{4.2}$$

This leads to the following discrete version of (2.1) frequently encountered in the literature,

$$\begin{aligned} &\text{Minimize} \quad \int_{\Omega_h} u_h \, \mathrm{d}x \quad \text{w.r.t. } u_h \in S^1_0(\Omega_h) \text{ and the nodal positions in } \Omega_h \\ &\qquad\qquad \text{s.t.} \quad (4.2). \end{aligned} \tag{4.3}$$

We refer the reader to Gangl et al., 2015; Sturm, 2016; Schulz, Siebenborn, Welker, 2016; Schulz, Siebenborn, 2016 for examples of this procedure.

Let us denote by $J_h(\Omega_h)$ the reduced objective value in (4.3), i.e., $J_h(\Omega_h) = \int_{\Omega_h} u_h \, \mathrm{d}x$, where u_h is the unique solution of (4.2). In order to derive a discrete variant of the volume formulation (3.2) of the Eulerian derivative, we introduce the discrete adjoint equation,

$$\text{Find } p_h \in S^1_0(\Omega_h) \quad \text{such that} \quad \int_{\Omega_h} \nabla p_h \cdot \nabla v_h \, \mathrm{d}x = -\int_{\Omega_h} v_h \, \mathrm{d}x \quad \text{for all } v_h \in S^1_0(\Omega_h). \tag{4.4}$$

The following theorem shows that a straightforward replacement of the state u and adjoint state p by their finite element equivalents u_h and p_h in (3.2) yields the correct formula for the Eulerian derivative $J_h'(\Omega_h; V_h)$ of the discrete objective J_h, provided that the perturbation field V_h is piecewise linear, i.e., V_h belongs to

$$S^1(\Omega_h)^d = \{u \in H^1(\Omega_h)^d : u\big|_T \in \mathcal{P}_1(T)^d \text{ for all cells } T \text{ in } \Omega_h\}. \tag{4.5}$$

THEOREM 4.1. *Suppose that u_h and p_h are the unique weak solutions of the discrete state equation* (4.2)*, and the discrete adjoint equation* (4.4)*, respectively. Moreover, let $V_h \in S^1(\Omega_h)^d$. Then*

$$\begin{aligned} J_h'(\Omega_h; V_h) &= \int_{\Omega_h} u_h \, (\operatorname{div} V_h) \, \mathrm{d}x \\ &+ \int_{\Omega_h} (\nabla u_h)^\top \left[(\operatorname{div} V_h) \operatorname{id} - DV_h - DV_h^\top\right] \nabla p_h \, \mathrm{d}x - \int_{\Omega_h} \operatorname{div}(f \, V_h) \, p_h \, \mathrm{d}x. \end{aligned} \tag{4.6}$$

The proof of this theorem follows along the lines of the continuous case, see, e.g., Hiptmair, Paganini, Sargheini, 2015; Laurain, Sturm, 2016. A detailed derivation can be found in Delfour, Payre, Zolesio, 1985, Section 4.

Remark 4.2.
1. Theorem 4.1 can be viewed as the statement that discretization and optimization (in the sense of forming the Eulerian derivative) commute for problem (2.1).
2. The finite element analogue of the *boundary expression* (3.4) is *not* an exact representation of the discrete Eulerian derivative. This is since the integration by parts necessary to pass from the volume to the boundary expression has to be done element by element and it leaves inter-element contributions; see also the discussion in Berggren, 2010.
3. Theorem 4.1 remains true when higher order Lagrangian finite elements on simplices are used in place of $S_0^1(\Omega_h)$. However it is essential that V_h remains piecewise linear so piecewise polynomials are transformed into piecewise polynomials of the same order.
4. Alternative expressions for (4.6) can be obtained following the so-called discrete adjoint approach, in which the derivative of $J_h(\Omega_h)$ w.r.t. the nodal positions of Ω_h is addressed by differentiating the finite element matrices. We refer to Schneider, Jimack, 2008; Berggren, 2010; Roth, Ulbrich, 2013 for examples of this procedure.

Despite the simplicity to obtain the Eulerian derivative of the discrete problem, we would like to emphasize here that the discrete problem (4.3) itself has the following serious drawback. The search space obtained from utilizing the nodal positions of the mesh Ω_h as optimization variables includes meshes with very degenerate cells. Those lead to poor approximations of solutions of the state equation, which may give rise, however, to smaller values of the discrete objective. Therefore, any optimization algorithm for the solution of (4.3) sooner or later is likely to encounter spurious descent directions which typically have support in only a few mesh nodes and which lead to degenerate meshes.

EXAMPLE 4.3. *Let us illustrate this behavior by means of problem* (2.1) *with data $f(x, y) = 2.5 \, (x + 0.4 - y^2)^2 + x^2 + y^2 - 1$. The optimal domain Ω is unknown. We* *begin with the computational mesh Ω_h shown in Figure 2 (left). Consider for example the piecewise linear vector field V_h represented by its nodal values*

$$V_h = \begin{cases} (-0.9510, -0.3090)^\top, & \text{for the node } v_0, \\ (0,0)^\top, & \text{for all other nodes} \end{cases}$$

where the boundary node v_0 can be easily identified from Figure 2.

We found that V is not only a descent direction for the objective at Ω_h but in fact that the line search function

$$t \mapsto J\big(T_t(\Omega_h)\big), \quad T_t = \mathrm{id} + t\, V_h$$

decreases until the triangle formed by v_0 and its two interior neighbors degenerates to a line, which happens at $t = 0.1$; see Figure 1. At this point, finite element computations break down.

In computational experience spurious descent directions do not usually occur during the early iterates. Thus they can be, and often are, avoided by early stopping, at the expense of a reduced tolerance. Alternatively, mesh quality control and remeshing can help to avoid mesh destruction, but this introduces discontinuities in the objective function's history.

In any case, the existence of spurious descent directions is a structural disadvantage of problem (4.3). Therefore we propose in the following section a new computational approach. Our approach does not seek to solve (4.3) literally but in a certain relaxed sense, which is inspired by the Hadamard structure theorem and which avoids spurious descent directions.

5. Restricted Mesh Deformations. By the Hadamard structure theorem, the Eulerian derivative for the continuous problem consists of normal boundary forces only, see (3.4) above. This is no longer the case for the discrete problem. The reason is that the finite element solutions u_h and p_h are only of limited regularity, and thus a global integration by parts necessary to pass from the volume expression (4.6) to a boundary expression is not available. This has been pointed out, for instance, in Delfour, Zolésio, 2011, note on p. 562. Therefore, we are going to continue with the discretely exact volume expression (4.6) but mimic the behavior of the continuous setting in the evaluation of the shape gradient, where we alloy only for shape displacements which are induced by normal forces.

5.1. Continuous Setting. To illustrate the situation, we start by discussing the continuous case. We have seen in (3.2) that the Eulerian derivative $J'(\Omega;\cdot)$ is an element of a dual space, e.g. an element of $(W^{1,\infty}(\Omega)^d)^\star$. In order to utilize this information for moving the domain Ω, we have to convert this dual element into a proper function. We follow the approach of Schulz, Siebenborn, Welker, 2016. To this end, we introduce the elasticity operator $E : H^1(\Omega)^d \to (H^1(\Omega)^d)^\star$ via

$$\langle E\, V, W\rangle := \int_\Omega 2\,\mu\,\boldsymbol{\varepsilon}(V) : \boldsymbol{\varepsilon}(W) + \lambda \operatorname{trace}(\boldsymbol{\varepsilon}(V)) \operatorname{trace}(\boldsymbol{\varepsilon}(W)) + \delta\, V \cdot W \,\mathrm{d}x \tag{5.1}$$

for all $V, W \in H^1(\Omega)^d$. Here and throughout, D denotes the derivative (Jacobian) of a vector valued function, $\boldsymbol{\varepsilon}(V) = (DV + DV^\top)/2$ is the linearized strain tensor, μ, λ are

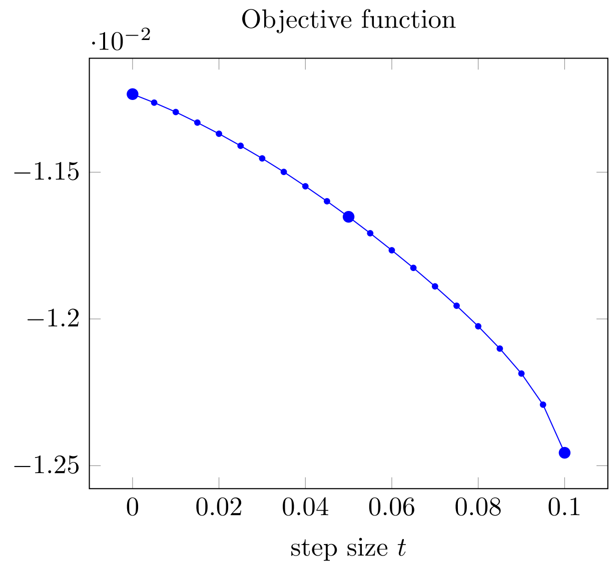

Fig. 1: $t \mapsto J\big(T_t(\Omega_h)\big)$ for Example 4.3. The step sizes $t = 0.00$, $t = 0.05$, $t = 0.10$ belonging to the domains in Figure 2 are highlighted.

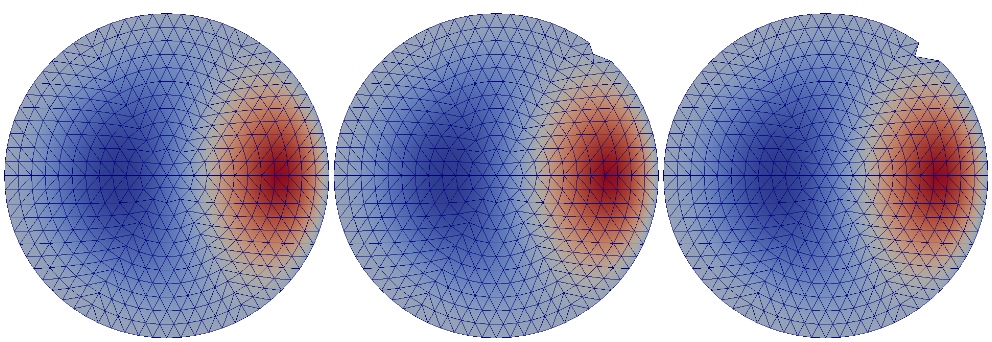

Fig. 2: Evolution of the mesh under $t \mapsto T_t(\Omega_h)$ with perturbation field V_h given in Example 4.3 at $t = 0.00$, $t = 0.05$, $t = 0.10$ (from left to right). The solutions u_h of the state equation (4.2) are also shown.

the Lamé parameters and $\delta > 0$ is a damping term. We assume $\mu > 0$, $d\,\lambda + 2\,\mu > 0$ so that E becomes positive semi-definite on $H^1(\Omega)^d$. Note that we do not consider Dirichlet boundary conditions in the space $H^1(\Omega)^d$. Therefore a positive damping parameter $\delta > 0$ is needed to ensure the coercivity of E, i.e., $\langle E\,V,\, V\rangle \ge \underline{c}\,\|V\|^2_{H^1(\Omega)^d}$ with some $\underline{c} > 0$. This result is due to Korn's inequality, see for instance Attouch, Buttazzo, Michaille, 2014, Proposition 6.6.1. Thus, E is an isomorphism and it furnishes $H^1(\Omega)^d$ with an inner product $(V,\, W)_E \coloneqq \langle E\,V,\, W\rangle$ so that E becomes the associated Riesz isomorphism.

In order to avoid technical regularity issues, we assume that the Eulerian derivative (3.2) enjoys the higher regularity $J'(\Omega;\cdot) \in (H^1(\Omega)^d)^\star$. This holds, e.g., if Ω is sufficiently smooth, due to the higher regularity of u and p. In order to compute the negative shape gradient w.r.t. the E-inner product on the continuous level, we solve

$$\text{Minimize} \quad J'(\Omega; V) + \frac{1}{2}\langle EV, V\rangle \quad \text{s.t. } V \in H^1(\Omega)^d. \tag{5.2}$$

The solution of this problem yields the negative shape gradient

$$V_{\text{grad}} := -E^{-1} J'(\Omega; \cdot). \tag{5.3}$$

Now, we introduce the normal force operator $N : L^2(\partial\Omega) \to (H^1(\Omega)^d)^\star$ given by

$$\langle NF, V\rangle = \int_{\partial\Omega} F\,(V \cdot \nu)\,\mathrm{d}s \tag{5.4}$$

for all $F \in L^2(\partial\Omega)$ and $V \in H^1(\Omega)^d$. Using again (3.4), we find that $J'(\Omega; \cdot)$ can be written as $J'(\Omega; \cdot) = N g_\Omega$ with

$$g_\Omega = -\frac{\partial u}{\partial \nu}\frac{\partial p}{\partial \nu} \in L^2(\partial\Omega).$$

Therefore, it is easy to see that problem (5.2) is equivalent to

$$\begin{aligned} \text{Minimize} \quad & J'(\Omega; V) + \frac{1}{2}\langle EV, V\rangle \\ \text{with respect to} \quad & V \in H^1(\Omega)^d, F \in L^2(\partial\Omega) \\ \text{such that} \quad & E\,V - N\,F = 0. \end{aligned} \tag{5.5}$$

Indeed, the additional constraint $E\,V - N\,F = 0$ is automatically satisfied by the unconstrained solution of (5.2). However, we will see that this property is lost after discretization, i.e., the discrete counterparts of (5.2) and (5.5) are going to differ. Note that the solution (V, F) of (5.5) is unique due to coercivity of E and injectivity of N. Moreover, since $\begin{bmatrix} E & -N \end{bmatrix}$ is surjective, there exists a unique Lagrange multiplier $\Pi \in H^1(\Omega)^d$ associated with the constraint $E\,V - N\,F = 0$; see for instance Luenberger, 1969, Chapter 9.3, Theorem 1. We therefore obtain the following necessary and sufficient optimality conditions for (5.5) in saddle-point form,

$$\begin{pmatrix} E & 0 & E \\ 0 & 0 & -N^\star \\ E & -N & 0 \end{pmatrix} \begin{pmatrix} V \\ F \\ \Pi \end{pmatrix} = \begin{pmatrix} -J'(\Omega; \cdot) \\ 0 \\ 0 \end{pmatrix}. \tag{5.6}$$

Here, $N^\star : H^1(\Omega)^d \to L^2(\partial\Omega)$ is the adjoint of N, where we identified $L^2(\partial\Omega)$ with its dual space. The multiplier Π in (5.6) necessarily satisfies $\Pi = 0$ since E is bijective. Now, it is easy to see that (5.6) is equivalent to solving

$$\begin{pmatrix} 0 & N^\star \\ N & E \end{pmatrix} \begin{pmatrix} F \\ \Pi \end{pmatrix} = \begin{pmatrix} 0 \\ -J'(\Omega; \cdot) \end{pmatrix}, \tag{5.7a}$$

$$V = -E^{-1} J'(\Omega; \cdot) - \Pi. \tag{5.7b}$$

Recall that $-E^{-1} J'(\Omega; \cdot)$ is the usual negative shape gradient w.r.t. E (i.e., the solution of (5.2)), whereas $-\Pi$ is a correction in order to obtain a shape displacement in the subspace $\operatorname{im}(E^{-1}N)$. Again, we emphasize that we have $\Pi = 0$ in the continuous setting, due to $-J'(\Omega;\cdot) = -N\, g_\Omega$. Therefore, the solution of (5.7) is just the usual shape gradient $V_{\text{grad}} = -E^{-1} J'(\Omega;\cdot)$.

Before discussing the discretized setting, we note that (5.5) is equivalent to

$$\begin{aligned} &\text{Minimize} && \frac{1}{2}\left\langle E(V - V_{\text{grad}}),\, V - V_{\text{grad}}\right\rangle \\ &\text{with respect to} && V \in H^1(\Omega)^d, F \in L^2(\partial\Omega) \\ &\text{such that} && E\,V - N\,F = 0. \end{aligned} \tag{5.8}$$

Hence, the solution V is the orthogonal projection (w.r.t. the inner product induced by E) of the usual shape gradient $V_{\text{grad}} = -E^{-1}J'(\Omega;\cdot)$ into the space $\operatorname{im}(E^{-1}N)$, i.e., the space of deformations induced by normal forces. This motivates to denote the solution of (5.5) by $V_{\text{proj grad}}$.

5.2. Discretized Setting. Next, we discuss the discretized setting. We refer to section 4 above for the introduction of the finite-element discretization. In addition to the FE space $S_0^1(\Omega_h) \subset H_0^1(\Omega_h)$, we recall from (4.5) the discrete space of mesh deformations

$$S^1(\Omega_h)^d = \{u \in H^1(\Omega_h)^d : u\big|_T \in \mathcal{P}_1(T)^d \text{ for all cells } T \text{ in } \Omega_h\}$$

and the boundary space

$$S^1(\partial\Omega_h) = \{u \in C(\partial\Omega_h)^d : u\big|_E \in \mathcal{P}_1(E)^d \text{ for all edges } E \text{ on } \partial\Omega_h\}. \tag{5.9}$$

We recall that the discrete Eulerian derivative $J_h'(\Omega_h;\cdot) \in (S^1(\Omega_h)^d)^\star$ was given in (4.6). Moreover, the discretization directly leads to the discretized operators $E_h : S^1(\Omega_h)^d \to (S^1(\Omega_h)^d)^\star$, $N_h : S^1(\partial\Omega_h) \to (S^1(\Omega_h)^d)^\star$ which are defined via

$$\begin{aligned} \langle E_h\, V_h,\, W_h\rangle &:= \int_{\Omega_h} 2\,\mu\,\boldsymbol{\varepsilon}(V_h) : \boldsymbol{\varepsilon}(W_h) + \lambda \operatorname{trace}(\boldsymbol{\varepsilon}(V_h)) \operatorname{trace}(\boldsymbol{\varepsilon}(W_h)) + \delta\, V_h \cdot W_h \,\mathrm{d}x, \\ \langle N_h\, F_h,\, V_h\rangle &:= \int_{\partial\Omega_h} F_h\,(V_h \cdot \nu)\,\mathrm{d}s \end{aligned}$$

for all $V_h, W_h \in S^1(\Omega_h)^d$ and $F_h \in S^1(\partial\Omega_h)$. Next, we will investigate the discrete counterparts of (5.2) and (5.5). The straightforward discretization of (5.2) reads

$$\text{Minimize} \quad J_h'(\Omega_h; V_h) + \frac{1}{2}\,\langle E_h V_h,\, V_h\rangle. \tag{5.10}$$

We denote its unique solution by $V_{\text{grad},h}$.

The important difference to the continuous case is that Hadamard's structure theorem is not available. The reason is that the discrete state u_h has only the limited regularity $u_h \in H_0^1(\Omega_h)$ and this regularity is not enough to transform the domain integral into a boundary integral via integration by parts, see the last paragraph in chapter 10, section 5.6 of Delfour, Zolésio, 2011. Therefore, unlike in the continuous case, $J_h'(\Omega_h;\cdot)$ does not belong, in general, to the image space of N_h. Consequently, the solution V_h of (5.10) has contributions not only from normal forces in the Eulerian derivative $J_h'(\Omega_h;\cdot)$, but also from interior forces as well as tangential boundary forces. Numerical examples in section 6 will show that these interior and tangential forces are responsible for spurious descent directions, which in turn lead to degenerate meshes.

Therefore, we conclude that it is not reasonable to try to solve

$$\text{Minimize } J_h(\Omega_h)$$

or its stationarity condition

$$\text{Find a triangulation } \Omega_h \text{ such that } V_{\text{grad},h} = -E_h^{-1} J_h'(\Omega_h;\cdot) = 0 \tag{5.11}$$

as a discretization of the continuous problem (1.1).

Hence, we consider the discretization of (5.5)

$$\begin{aligned} &\text{Minimize} && J_h'(\Omega_h;V_h) + \frac{1}{2}\langle E_h V_h,\, V_h\rangle \\ &\text{with respect to} && V_h \in S^1(\Omega_h)^d, F_h \in S^1(\partial\Omega_h) \\ &\text{such that} && E_h\, V_h - N_h\, F_h = 0. \end{aligned} \tag{5.12}$$

in which we restrict $E\, V_h$ to the image space of the discrete normal force operator N_h. As in the continuous setting, this problem is equivalent to the solution of

$$\begin{pmatrix} E_h & 0 & E_h \\ 0 & 0 & -N_h^\star \\ E_h & -N_h & 0 \end{pmatrix} \begin{pmatrix} V_h \\ F_h \\ \Pi_h \end{pmatrix} = \begin{pmatrix} -J_h'(\Omega_h;\cdot) \\ 0 \\ 0 \end{pmatrix}. \tag{5.13}$$

It is clear that (5.13) can also be reduced as in (5.7). For later reference, we mention that the solution $(V_{\text{proj grad},h}, F_h, \Pi_h)$ of (5.13) satisfies

$$\begin{aligned} \langle E_h\, V_{\text{proj grad},h},\, V_{\text{proj grad},h}\rangle &= -\langle E_h\, V_{\text{proj grad},h},\, \Pi_h\rangle - J_h'(\Omega_h; V_{\text{proj grad},h}) \\ &= -\langle N_h\, F_h,\, \Pi_h\rangle - J_h'(\Omega_h; V_{\text{proj grad},h}) \\ &= -J_h'(\Omega_h; V_{\text{proj grad},h}) \end{aligned} \tag{5.14}$$

since $N_h^\star\, \Pi_h = 0$ holds. This shows that $V_{\text{proj grad},h}$ is always a descent direction for the discrete objective $J_h(\Omega_h;\cdot)$.

As we have seen in (5.8) for the continuous setting, the solution V_h of (5.12) also solves

$$\begin{aligned} &\text{Minimize} && \frac{1}{2}\big\langle E_h(V_h - V_{\text{grad},h}),\, V_h - V_{\text{grad},h}\big\rangle \\ &\text{with respect to} && V_h \in S^1(\Omega_h)^d, F_h \in S^1(\partial\Omega_h) \\ &\text{such that} && E_h\, V_h - N_h\, F_h = 0, \end{aligned} \tag{5.15}$$

where $V_{\text{grad},h} = -E_h^{-1} J_h'(\Omega_h;\cdot)$ is the solution of (5.10). Again, the solution $V_{\text{proj grad},h}$ of (5.15) can be interpreted as the projection (w.r.t. the E_h inner product) of $V_{\text{grad},h}$ onto the image space of $E_h^{-1} N_h$. Therefore, the notation $V_{\text{proj grad},h}$ for the solution of (5.12) is justified.

Our main idea is now to propose, instead of (5.11),

$$\text{Find a triangulation } \Omega_h \text{ such that } V_{\text{proj grad},h} = 0 \tag{5.16}$$

as an appropriate discrete version of (1.1). Note that this is fundamentally different from the ad-hoc discretization (5.11) since we neglect the contributions of $J_h'(\Omega_h;\cdot)$

which do not belong to the image space of N_h. We will see via numerical examples that this problem (5.16) can be solved to high accuracy by an iterative algorithm using the solution $V_{\text{proj grad},h}$ of (5.12) for the displacement of the triangulation Ω_h (together with a line-search). Moreover, we will see that the solutions Ω_h converge to a stationary point of the continuous problem (1.1) under suitable assumptions when successively finer meshes are used; see section 9 below.

For later use, we are going to characterize stationarity of Ω_h in the sense of (5.16). The deformation $V_h = 0$ solves the projection problem (5.15) if and only if

$$\langle E_h \, V_{\text{grad},h}, \, E_h^{-1} \, N_h \, F_h \rangle = 0 \qquad \forall F_h \in S^1(\partial\Omega_h).$$

This, in turn, is equivalent to

$$\int_{\partial\Omega_h} F_h \, (V_{\text{grad},h} \cdot \nu) \, \mathrm{d}s = 0 \qquad \forall F_h \in S^1(\partial\Omega_h). \tag{5.17}$$

This means that Ω_h is stationary in the sense of (5.16) if and only if the usual shape gradient $V_{\text{grad},h}$ is a tangential vector field on Ω_h in a discrete sense.

We can now state a restricted gradient algorithm for the solution of (5.16), where we use $V_{\text{proj grad},h}$ as the deformation field which provides the search direction in the domain transformation. It is sufficient to utilize a simple a backtracking strategy to comply with the Armijo condition

$$J_h\big((\mathrm{id} + t\, V_{\text{proj grad},h})(\Omega_h)\big) \le J_h(\Omega_h) + \sigma \, t \, J_h'(\Omega_h; V_{\text{proj grad},h}). \tag{5.18}$$

Here, $\sigma \in (0,1)$ is a parameter.

Since we are using the perturbation of identity approach (1.2) instead of a more sophisticated family of domain transformations, we also perform a mesh quality control in order to avoid gradient steps which are too large. To this end, we check that the conditions

$$\frac{1}{2} \le \det(\mathrm{id} + t\, DV_{\text{proj grad},h}) \le 2, \qquad \|t\, DV_{\text{proj grad},h}\|_F \le 0.3 \tag{5.19}$$

are satisfied in every cell throughout the entire domain. Here, $\|\cdot\|_F$ denotes the Frobenius norm of matrices. The first condition monitors the change of volume of the cell, while the second additionally inhibits large changes of the angles. Note that this amounts to checking three inequalities per cell. Due to (5.14), we use

$$\langle E_h V_{\text{proj grad},h}, \, V_{\text{proj grad},h} \rangle = -J_h'(\Omega_h; V_{\text{proj grad},h}) \le \varepsilon_{\text{tol}}^2 \tag{5.20}$$

as a convergence criterion for some small $\varepsilon_{\text{tol}} > 0$. These considerations lead to Algorithm 1.

6. Numerical Results: Restricted vs. Classical Gradient Method. The main goal of this section is to compare our proposed restricted gradient method, see Algorithm 1, to a classical shape gradient method. The latter is identical to Algorithm 1 except that $V_{\text{proj grad},h}$ is replaced everywhere by the negative shape gradient $V_{\text{grad},h}$ from (5.10). We consider our model problem (2.1) with data f as in Example 4.3. The line-search parameters $\beta = 0.5$ and $\sigma = 0.1$ are used. The initial shape for both methods is the same as in Figure 2 (left).

Algorithm 1: Restricted gradient method for (5.16).

```
Data: Initial domain Ω_h
Initial step size t, convergence tolerance ε_tol,
Line-search parameters β ∈ (0,1), σ ∈ (0,1)
Result: Improved domain Ω_h on which (5.16) holds up to ε_tol
for i ← 1 to ∞ do
    Solve the discrete state equation (4.2) for u_h;
    Solve the discrete adjoint equation (4.4) for p_h;
    Solve (5.12) for V_{proj grad,h} with shape derivative J'(Ω_h; ·) from (4.6);
    if ⟨E_h V_{proj grad,h}, V_{proj grad,h}⟩ ≤ ε_tol^2 then
        STOP, the current iterate Ω_h is almost stationary for (5.16);
    end
    Increase step size t ← t/β;
    while (5.18) or (5.19) is violated do
        Decrease step size t ← β t;
    end
    Transform the domain according to Ω_h ← (id + t V_{proj grad,h})(Ω_h);
end
```

We implemented Algorithm 1 and its classical counterpart in FEniCS, version 2018.1 (Logg, Mardal, Wells, et al., 2012). All derivatives were automatically generated by the built-in algorithmic differentiation capabilities. The restricted shape gradient $V_{\text{proj grad},h}$, i.e., the solution of (5.12), was computed via the discrete counterpart of (5.7). The linear system was solved using SciPy's `spsolve` with the SuperLU solver (Li, 2005), i.e., with the setting `use_umfpack = False`.

The restricted gradient method reached the desired tolerance

$$\|V_{\text{proj grad},h}\|_{E_h} \le \varepsilon_{\text{tol}} = 10^{-7}$$

at iteration 858, while the classical gradient method was stopped at iteration 1000, where it had only reached

$$\|V_{\text{grad},h}\|_{E_h} \approx 7 \cdot 10^{-3}.$$

Figures 4 and 5 show the complete history of the objective and respective shape gradient norms.

Figure 3 shows the domains Ω_h during the iteration of both methods for comparison. It can clearly be inferred that the initial iterates are virtually identical but both methods begin to produce visibly different shapes around iteration 500, when the objective value (shown in Figure 4) has practically converged but the gradient norms are still

$$\|V_{\text{grad},h}\|_{E_h} \approx 5 \cdot 10^{-3} \quad \text{and} \quad \|V_{\text{proj grad},h}\|_{E_h} \approx 4 \cdot 10^{-6},$$

respectively. At this point, the classical gradient method starts to pursue spurious descent directions, which results in a further decrease of the discrete objective at the expense of increasingly degenerate meshes.

To further illustrate this point, we show in Figure 6 visualizations of the Eulerian derivative $J_h'(\Omega_h; \cdot)$ for both methods; see (4.6). In fact, this is a linear functional on

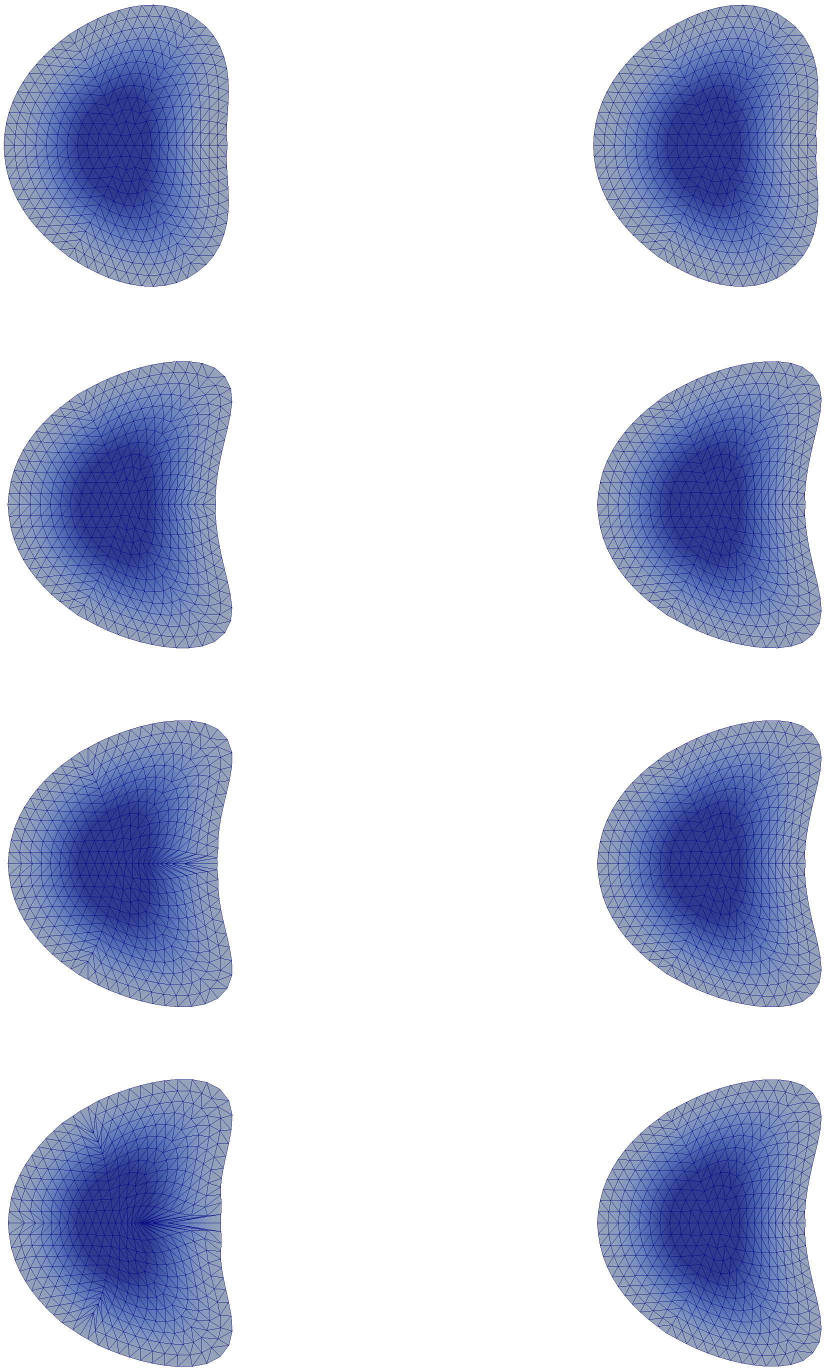

Fig. 3: Intermediate shapes Ω_h obtained with the classical gradient method (left) and the restricted gradient method (right) at iterations 5, 300, 600, 900.

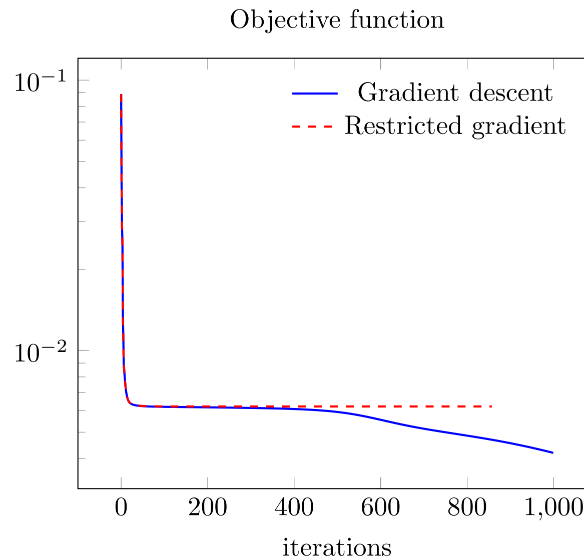

Fig. 4: History of the objective value $J_h(\Omega_h)$ along the iterations.

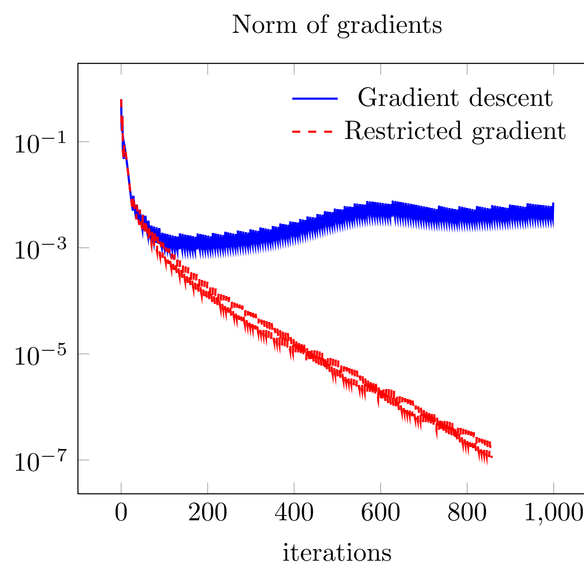

Fig. 5: History of the norm of the gradients $\|V_{\mathrm{grad},h}\|_{E_h}$ (for the gradient descent method) and $\|V_{\mathrm{proj\,grad},h}\|_{E_h}$ (for the restricted gradient method) along the iterations.

the space of piecewise linear perturbation fields $V_h \in S^1(\Omega_h)^d$. In Figure 6 we display the $S^1(\Omega_h)^d$ representer of $J_h'(\Omega_h; \cdot)$ w.r.t. the L^2 inner product, i.e., we solve a linear system governed by a block-diagonal mass matrix.

Let us comment on the Eulerian derivative for the restricted gradient method as shown in the right column of Figure 6. It is apparent that the displacement field

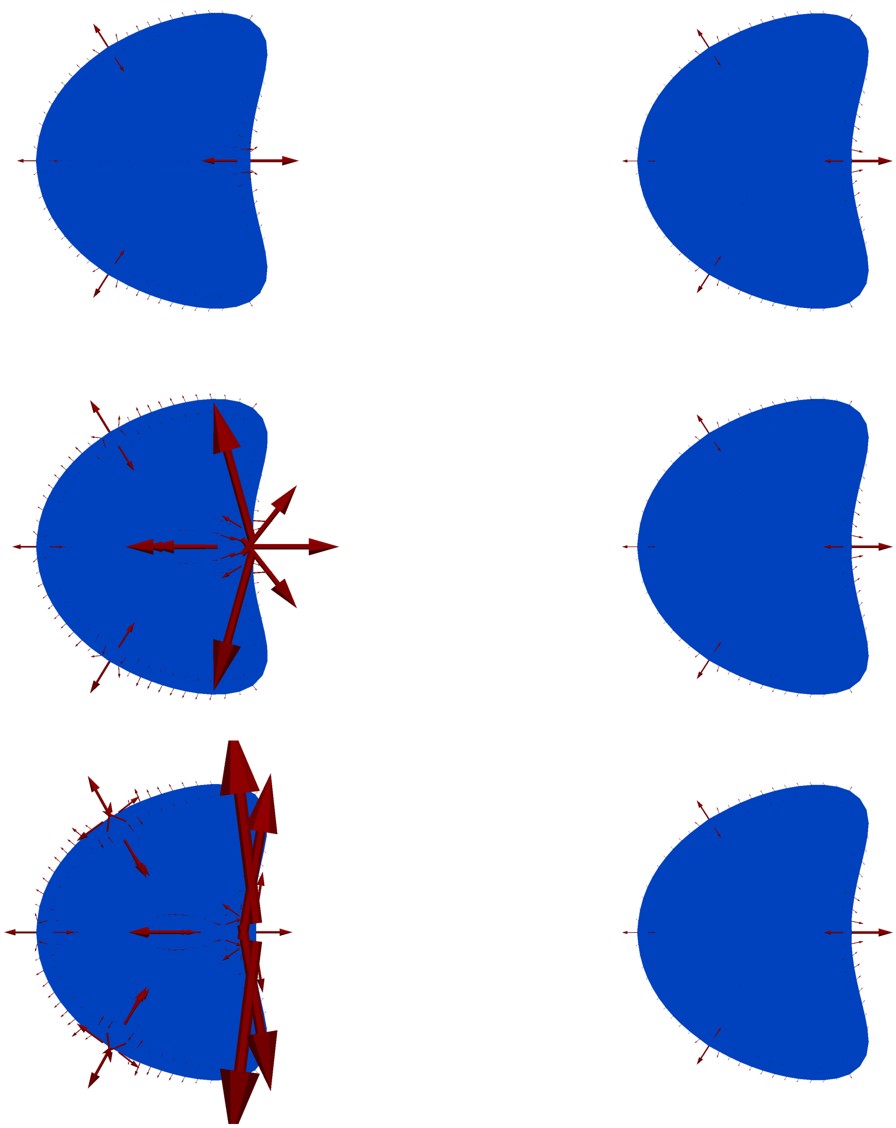

Fig. 6: Visualization of the Eulerian derivatives $J_h'(\Omega_h; \cdot)$ obtained with the classical gradient method (left) and the restricted gradient method (right) at iterations 300, 600, 900 (top to bottom).

$V_{\mathrm{grad},h}$, i.e., the solution of (5.10), is non-zero and in fact essentially the same for the iterations 300, 600, and 900 shown. However $V_{\mathrm{grad},h}$ also has essentially no component in the space of deformations induced by normal forces. Therefore its projection into this space, see (5.15), leaves us with a very small norm $\|V_{\mathrm{proj\,grad},h}\|_{E_h}$, as shown in Figure 5. The images visualizing the Eulerian derivative for the classical gradient method in the left column of Figure 6 show that the method has allowed the spurious part of the derivative to build up, which eventually dominates the search direction.

7. Restricted Newton-Like Method. In the previous two sections we have seen that (5.16) is a reasonable discrete optimality condition and that it can be solved to high accuracy via a first-order gradient descent method. However, as is well known for the minimization of even mildly ill-conditioned quadratic polynomials, gradient descent methods require a large number of iterations to achieve convergence. We observed the same behavior in section 6.

Therefore, we are also investigating a Newton-like method for solving (5.16). First, we focus on the continuous case and comment on its discretization afterwards. Let Ω be our current iterate. As before, we denote by u the associated state, see (2.2), and by p the adjoint state, see (3.3). The solution of the restricted shape gradient problem (5.6) at Ω is denoted by $(V_{\text{proj grad}}, F, \Pi)$. Recall that our goal is to achieve $V_{\text{proj grad}} = 0$ or, equivalently, $F = 0$, cf. (5.16). In practice, we impose a stopping criterion of the form $\|V_{\text{proj grad}}\|_E \le \varepsilon_{\text{tol}}$ as we did for the gradient method.

In order to allow the reader to follow the derivation for the solution of (5.16) of our Newton method more easily, we draw the parallel with Newton's method for $\Phi(x) = 0$ for some $\Phi : \mathbb{R}^n \to \mathbb{R}^n$. We consider the equation $\Phi(x + \delta x) = 0$ for the unknown update δx. In our context the iterate x represents the current domain Ω and the update corresponds to a perturbation field W. Since the update takes Ω into a new domain, we need to manipulate the expression $\Phi(x + \delta x) = 0$ and pull it back to Ω. Finally, we linearize about $\delta x = 0$, which amounts to $\Phi(x) + D\Phi(x)\,\delta x = 0$.

In our Newton method we seek a deformation field W (taking the role of δx above) such that the updated domain $\Omega_W := (\mathrm{id} + W)(\Omega)$ is stationary in the sense that the solution of (5.6) (at Ω_W instead of Ω) satisfies $V^W_{\text{proj grad}} = 0$. As in section 5 we are only considering updates W which are induced by a normal force G, i.e., $E\,W - N\,G = 0$ should hold.

In order to characterize the stationarity of the transformed domain Ω_W, we introduce the elasticity operator $E_W : H^1(\Omega_W)^d \to (H^1(\Omega_W)^d)^\star$ and the normal force operator $N_W : L^2(\partial\Omega_W) \to (H^1(\Omega_W)^d)^\star$ on Ω_W analogously to (5.1) and (5.4). With the transformation field $T_W := \mathrm{id} + W : \Omega \to \Omega_W$, we define the pullbacks $E^W : H^1(\Omega)^d \to (H^1(\Omega)^d)^\star$ of E_W and $N^W : L^2(\partial\Omega) \to (H^1(\Omega)^d)^\star$ of N_W via

$$
\begin{aligned}
\langle E^W\, W_1,\, W_2\rangle &:= \langle E_W\,(W_1 \circ T_W^{-1}),\, W_2 \circ T_W^{-1}\rangle,\\
\langle N^W\, F,\, W\rangle &:= \langle N_W\,(F \circ T_W^{-1}),\, W \circ T_W^{-1}\rangle
\end{aligned}
$$

for $W_1, W_2, W \in H^1(\Omega)^d$.

Since we wish to achieve conditions defined on the current domain Ω, rather than on the unknown transformed domain Ω_W after the Newton step, we consider the Lagrangian associated with problem (2.1) on $\Omega_W = T_W(\Omega)$ and pull it back to Ω. Using the usual integral substitution and chain rule, and denoting the pulled-back solutions of the state and adjoint equations on Ω_W by u^W and p^W, respectively, we obtain $\mathcal{L} : W^{1,\infty}(\Omega)^d \times H_0^1(\Omega) \times H_0^1(\Omega) \to \mathbb{R}$, defined as

$$\begin{aligned}\mathcal{L}(W, u^W, p^W) &= \int_\Omega u^W \det(\mathrm{id} + DW)\,\mathrm{d}x \\ &\quad + \int_\Omega ((\mathrm{id} + DW)^{-\top} \nabla u^W) \cdot ((\mathrm{id} + DW)^{-\top} \nabla p^W) \det(\mathrm{id} + DW)\,\mathrm{d}x \\ &\quad - \int_\Omega (f \circ T_W) \det(\mathrm{id} + DW)\,\mathrm{d}x.\end{aligned}$$

Notice that $\frac{\partial}{\partial W}\mathcal{L}(W, u^W, p^W)$ is the shape derivative $J'(\Omega_W; \cdot)$. Thus we find that the stationarity of Ω_W is equivalent to the requirement that the solution of the nonlinear system

$$\begin{pmatrix} \cdot & \cdot & \cdot & \cdot & \cdot \\ \cdot & \cdot & \cdot & \cdot & \cdot \\ \cdot & \cdot & E^W & \cdot & E^W \\ \cdot & \cdot & \cdot & \cdot & -(N^W)^\star \\ \cdot & \cdot & E^W & -N^W & \cdot \end{pmatrix} \begin{pmatrix} u^W \\ p^W \\ V^W_{\text{proj grad}} \\ F^W \\ \Pi^W \end{pmatrix} + \begin{pmatrix} \frac{\partial}{\partial u}\mathcal{L}(W, u^W, p^W) \\ \frac{\partial}{\partial p}\mathcal{L}(W, u^W, p^W) \\ \frac{\partial}{\partial W}\mathcal{L}(W, u^W, p^W) \\ \cdot \\ \cdot \end{pmatrix} = 0$$

satisfies $V^W_{\text{proj grad}} = 0$. In view of the injectivity of N^W, this is equivalent to $F^W = 0$. Here, "$\cdot$" stands for a zero block. We mention that the first two equations in this system correspond to the adjoint and state equation on Ω_W but pulled back to Ω, respectively. Moreover, note that the solution $(u^W, p^W, V^W_{\text{proj grad}}, F^W, \Pi^W)$ of the above system is the pull-back of the solution of the state equation, adjoint equation and the projected shape gradient of the system (5.6) formulated on the domain Ω_W.

Together with the requirement that the deformation field W itself is induced by some normal force G, we have to solve the nonlinear system

(7.1)
$$\begin{pmatrix} \cdot & \cdot & \cdot & \cdot & \cdot & \mathrm{id} & \cdot \\ E & -N & \cdot & \cdot & \cdot & \cdot & \cdot \\ \cdot & \cdot & \cdot & \cdot & \cdot & \cdot & \cdot \\ \cdot & \cdot & \cdot & \cdot & \cdot & \cdot & \cdot \\ \cdot & \cdot & \cdot & \cdot & E^W & \cdot & E^W \\ \cdot & \cdot & \cdot & \cdot & \cdot & \cdot & -(N^W)^\star \\ \cdot & \cdot & \cdot & \cdot & E^W & -N^W & \cdot \end{pmatrix} \begin{pmatrix} W \\ G \\ u^W \\ p^W \\ V^W_{\text{proj grad}} \\ F^W \\ \Pi^W \end{pmatrix} + \begin{pmatrix} \cdot \\ \cdot \\ \frac{\partial}{\partial u}\mathcal{L}(W, u^W, p^W) \\ \frac{\partial}{\partial p}\mathcal{L}(W, u^W, p^W) \\ \frac{\partial}{\partial W}\mathcal{L}(W, u^W, p^W) \\ \cdot \\ \cdot \end{pmatrix} = 0.$$

As before, N and E denote the normal force operator and the elasticity operator on Ω.

The system (7.1) for W and the further, auxiliary unknowns corresponds to the nonlinear system $\Phi(x + \delta x) = 0$ for the step δx. For convenience, we recall the meaning of the seven equations in (7.1). The first equation requires $F^W = 0$, i.e., the stationarity of the updated domain Ω_W. The second equation is the requirement that the displacement W is induced by the (normal) force G. The third and fourth equation are the adjoint and state equation on Ω_W. Finally, the last three equations are the pullback of the system (5.6) on Ω_W to Ω.

We can now describe a step of our Newton-like procedure for the solution of the nonlinear system (7.1). Suppose that Ω is the current domain and consider an iterate of the form $(0, 0, u, p, V_{\text{proj grad}}, F, \Pi)$ with the state, the adjoint state, and the solution of (5.6) on Ω. Notice that for this iterate, the residual of (7.1) is $(F, 0, 0, 0, 0, 0, 0)$.

Next we linearize the system (7.1) about this current iterate w.r.t. all seven variables. We refrain from stating the lengthy formula for the linear system which results. In practice, we generate this linear system governing the Newton step using the algorithmic differentiation capabilities of FEniCS (Logg, Mardal, Wells, et al., 2012). From the solution of that linear system we only extract the Newton update for the perturbation field. We refer to it as W since its current value is zero. We then apply W to the current domain Ω to obtain the new domain $(\mathrm{id} + W)(\Omega)$. The six remaining variables are updated in a different fashion. Rather than using the solution from the Newton step, we solve again the state and adjoint state equations on the new domain, as well as the system (5.6) returning the projected shape gradient. This procedure can be understood as a Newton-like method with nonlinear updates for some of the variables. It ensures that the new iterate is of the same form as above. Moreover, it allows us access to the projected shape gradient and its norm in every iteration so that we can use $\|V_{\text{proj grad}}\|_E \le \varepsilon_{\text{tol}}$ as a stopping criterion as we did for the restricted gradient method.

Numerically, we have observed some instabilities if the current iterate Ω is far from being stationary. Moreover we wish to establish a step size control in order to monitor the Armijo condition (5.18) and the mesh quality condition (5.19). To this end we added a regularization term $-G/t$ to the first equation of (7.1), i.e., we obtain

(7.2)
$$\begin{pmatrix} \cdot & -t^{-1}\mathrm{id} & \cdot & \cdot & \cdot & \mathrm{id} & \cdot \\ E & -N & \cdot & \cdot & \cdot & \cdot & \cdot \\ \cdot & \cdot & \cdot & \cdot & \cdot & \cdot & \cdot \\ \cdot & \cdot & \cdot & \cdot & \cdot & \cdot & \cdot \\ \cdot & \cdot & \cdot & \cdot & E_W & \cdot & E_W \\ \cdot & \cdot & \cdot & \cdot & \cdot & \cdot & -N_W^\star \\ \cdot & \cdot & \cdot & \cdot & E_W & -N_W & \cdot \end{pmatrix} \begin{pmatrix} W \\ G \\ u \\ p \\ V_{\text{proj grad}} \\ F \\ \Pi \end{pmatrix} + \begin{pmatrix} \cdot \\ \cdot \\ \frac{\partial}{\partial u}\mathcal{L}(W,u,p) \\ \frac{\partial}{\partial p}\mathcal{L}(W,u,p) \\ \frac{\partial}{\partial W}\mathcal{L}(W,u,p) \\ \cdot \\ \cdot \end{pmatrix} = 0.$$

Thus, the update resulting from the solution of the Newton system satisfies $-t^{-1}\delta G + \delta F = -F$. Heuristically, this leads to $\delta G \approx t\,F$ for small t. Consequently, the transformation field which is applied to the current domain Ω satisfies $W = E^{-1}\,N\,\delta G \approx t\,V_{\text{proj grad}}$ is essentially a scaled (restricted) gradient direction for small t. Therefore, similar as in a Levenberg–Marquardt method, we will refer to t as the damping parameter and it serves the same purpose as the step length parameter in Algorithm 1.

A discrete variant of our Newton-like method is readily derived and given as Algorithm 2. In order to determine an appropriate damping parameter we consider analogues of the Armijo condition (5.18) and the mesh quality criterion (5.19). For the sake of clarity we re-state them with the relevant quantities for the Newton-like method. In particular, we use the step length $t = 1$ therein, since the scaling of the step is already realized by the damping in (7.2). The Armijo condition becomes

$$J_h\big((\mathrm{id} + W_h)(\Omega_h)\big) \le J_h(\Omega_h) + \sigma\, J_h'(\Omega_h; W_h). \tag{7.3}$$

with some parameter $\sigma \in (0, 0.5)$. The mesh quality criterion holds if

$$\frac{1}{2} \le \det(\mathrm{id} + DW_h) \le 2, \qquad \|DW_h\|_F \le 0.3. \tag{7.4}$$

is satisfied in every cell. In addition we verify that W_h yields a descent direction. If any of the above conditions fails, we decrease the damping parameter t.

Algorithm 2: Restricted Newton method for (5.16).

Data: Initial domain Ω_h
Initial damping parameter t, convergence tolerance ε_{tol},
Line-search parameters $\beta \in (0,1)$, $\sigma \in (0, 0.5)$
Result: Improved domain Ω_h on which (5.16) holds up to ε_{tol}

for $i \leftarrow 1$ **to** ∞ **do**
  Solve the discrete state equation (4.2) for u_h;
  Solve the discrete adjoint equation (4.4) for p_h;
  Solve (5.12) for $V_{\text{proj grad},h}$ with shape derivative $J_h'(\Omega_h; \cdot)$ from (4.6);
  if $\langle E_h V_{\text{proj grad},h},\, V_{\text{proj grad},h} \rangle \le \varepsilon_{\text{tol}}^2$ **then**
    STOP, the current iterate Ω_h is almost stationary for (5.16);
  end
  Increase damping parameter $t \leftarrow t/\beta$;
  Solve the Newton system associated with (7.2) with damping parameter t and extract the first component as W_h;
  while $J_h'(\Omega_h; W_h) \ge 0$ *holds, or* (7.3) *or* (7.4) *is violated* **do**
    Decrease damping parameter $t \leftarrow \beta\, t$;
    Solve the Newton system associated with (7.2) with damping parameter t and extract the first component as W_h;
  end
  Transform the domain according to $\Omega_h \leftarrow (\mathrm{id} + W_h)(\Omega_h)$;
end

8. Numerical Results: Newton-Like Method. This section is devoted to numerical results obtained by solving the same problem as in section 6 using the Newton-like method as described in section 7. For this approach the stopping criterion

$$\|V_{\text{proj grad},h}\|_{E_h} \le \varepsilon_{\text{tol}} = 10^{-9}$$

was satisfied after 12 iterations. Some of the intermediate shapes are shown in Figure 7. As was already mentioned, we have the linear system in each Newton step assembled using the algorithmic differentiation capabilities of FEniCS and solved in the same way as we did for the gradient method.

9. Convergence of Discrete Shapes. In this section we prove a result concerning the convergence of a sequence of discretely stationary domains Ω_n satisfying $V_{\text{proj grad},n} = 0$ to a stationary point Ω of the continuous problem satisfying $V_{\text{grad}} = V_{\text{proj grad}} = 0$ as the discretization mesh size goes to zero. This result is a further indication that our discretization (5.16) is reasonable.

To our knowledge, similar results are only available if the space of shapes is restricted to a class of parametrized shapes. In Eppler, Harbrecht, Schneider, 2007, the authors consider shapes in $\mathbb{R}^2$ which are star-shaped w.r.t. the origin. Consequently, this class of shapes is discretized using periodic splines and the boundary element method is employed for the state equation. Under appropriate assumptions, convergence of the discretization is proved. A similar approach is used in Kiniger, Vexler, 2013. Therein, the authors considered the optimization of the lower boundary of the unit square $(0,1)^2 \subset \mathbb{R}^2$. They employ a parametrization of this lower boundary and the entire problem is mapped back to the unit square $(0,1)^2$. The problem is discretized by finite

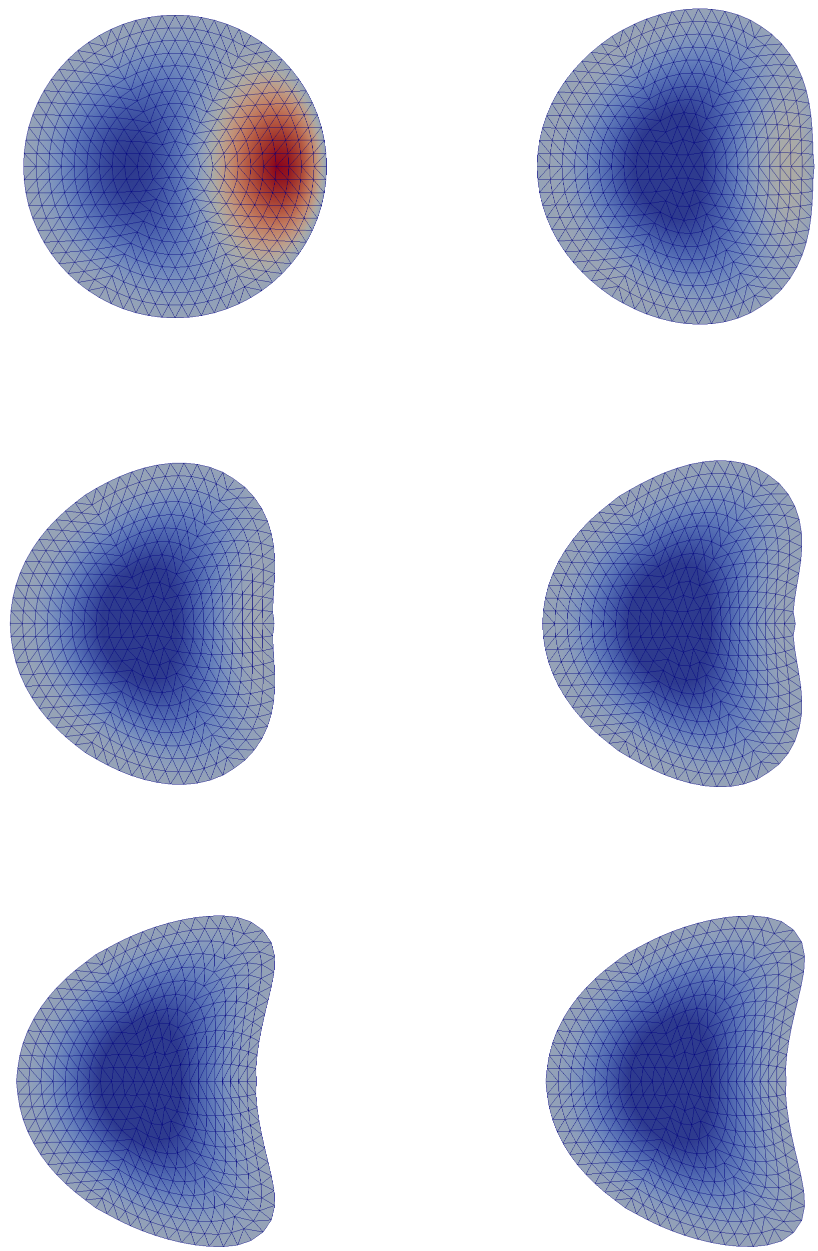

Fig. 7: Intermediate shapes Ω_h obtained with the restricted Newton method at iterations 0, 4, 5, 6, 9, 12.

elements and the convergence of this scheme is proven. The same technique is used in Fumagalli, Parolini, Verani, 2015 for shape optimization of Stokes flow. We emphasize that these three results also derive convergence rates.

As already said, we consider a sequence of triangulations. Note that we are going to solve (5.16) on each of these triangulations and the mesh deformations change the mesh width (which is usually denoted by h). Hence, we do not use the index h to refer to the triangulations, but we will just use $n \in \mathbb{N}$ as discretization parameter. In what follows, for all $n \in \mathbb{N}$, Ω_n will be a triangulated domain. For the purpose of this section we denote by

Next, we fix the assumptions which are necessary for our convergence result. To this end, we introduce the elasticity operator on Ω_n via

$$\langle E_n V, W \rangle := \int_{\Omega_n} 2\,\mu\,\boldsymbol{\varepsilon}(V) : \boldsymbol{\varepsilon}(W) + \lambda \operatorname{trace}(\boldsymbol{\varepsilon}(V)) \operatorname{trace}(\boldsymbol{\varepsilon}(W)) + \delta\, V \cdot W \,\mathrm{d}x \tag{9.1}$$

for all $V, W \in H^1(\Omega_n)^d$.

Assumption 9.1. *Suppose that $\{\Omega_n\}$ is a sequence of triangulations, each of which is stationary in the sense of (5.16). Moreover, let Ω be a domain of class $C^{1,1}$ and we assume the following.*

(A1) *The right-hand side f of the PDE satisfies $f \in W^{1,4}(D)$.*
(A2) *The maximum mesh width h_n in Ω_n goes to 0 as $n \to \infty$.*
(A3) *For arbitrary $g \in L^2(D)$ the FE solutions $w_n \in S^1_0(\Omega_n)$ of*

$$\int_{\Omega_n} \nabla w_n \cdot \nabla v_n \,\mathrm{d}x = \int_{\Omega_n} g\, v_n \,\mathrm{d}x \qquad \forall v_n \in S^1_0(\Omega)_n$$

extended by zero to all of D, converge in $W^{1,4}_0(D)$ towards (the zero extension of) the solution $w \in H^1_0(\Omega)$ of

$$-\Delta w = g \text{ in } \Omega, \quad w = 0 \text{ on } \partial\Omega.$$

(A4) *For arbitrary $G_0 \in L^2(D)^d$, $G_1 \in L^2(D)^{d\times d}$ the FE solutions $W_n \in S^1(\Omega_n)^d$ of*

$$\langle E_n W_n, V \rangle = \int_{\Omega_n} G_0 \cdot V_n + G_1 : DV_n \,\mathrm{d}x \qquad \forall V_n \in S^1(\Omega_n)^d$$

and the solution $W \in H^1(\Omega)^d$ of

$$\langle E\, W, V \rangle = \int_{\Omega} G_0 \cdot V + G_1 : DV \,\mathrm{d}x \qquad \forall V \in H^1(\Omega)^d$$

satisfy

$$\int_{\partial\Omega_n} (W_n \cdot \nu_n)\,\varphi \,\mathrm{d}s \to \int_{\partial\Omega} (W \cdot \nu)\,\varphi \,\mathrm{d}s \qquad \forall \varphi \in W^{1,\infty}(D),$$

where ν_n and ν denote the outer unit normal vectors on Ω_n and Ω, respectively.
(A5) *The trace operators from $H^1(\Omega_n)$ to $L^1(\partial\Omega_n)$ are uniformly bounded, independently of $n \in \mathbb{N}$.*

Remark 9.2. It would be nice to replace **(A3)** and **(A4)** by some more tractable conditions. One possibility is to use the geometric assumption

$$(\Omega_n \setminus \Omega) \cup (\Omega \setminus \Omega_n) \subset \{x \in \mathbb{R}^d \mid \operatorname{dist}(x, \partial\Omega) \le \varepsilon_n\}$$

with $\varepsilon_n \to 0$ and to assume that, additionally to **(A2)**, the aspect ratios of all triangles in $\{\Omega_n\}$ remain bounded as $n \to \infty$. With these assumptions it is possible to show that the FE solutions w_n converge to w in $H^1(D)$. However, it is not clear how to improve this convergence to convergence in $W^{1,4}(D)$. For this, it would, e.g., be sufficient to get a uniform bound for $\|w_n\|_{W^{1,\infty}}$, but this seems to be far from trivial. With similar arguments one is able to obtain **(A4)** from the above geometric assumption. For this, it is crucial to use

$$\int_{\partial\Omega_n} (W_n \cdot \nu_n)\, \varphi \,\mathrm{d}s = \int_{\Omega_n} \operatorname{div}(W_n\, \varphi)\,\mathrm{d}x, \qquad \int_{\partial\Omega} (W \cdot \nu)\, \varphi \,\mathrm{d}s = \int_{\Omega} \operatorname{div}(W\, \varphi)\,\mathrm{d}x$$

due to Gauß' divergence theorem.

Since we assumed that the hold-all D has a $C^{1,1}$ boundary, we have $C^{0,1}(\bar{D}) = W^{1,\infty}(D)$, see Delfour, Zolésio, 2011, Section 2.6.4.

First we remark that Assumption 9.1 implies the convergence of states and adjoints.

LEMMA 9.3. *Let us denote by u_n, p_n the discretized states and adjoints, i.e., the solutions of* (4.2) *and* (4.4)*, respectively, with h replaced by n. Similarly, u and p denote the state and adjoint associated with Ω. Then,*

$$\|u_n - u\|_{W_0^{1,4}(D)} + \|p_n - p\|_{W_0^{1,4}(D)} \to 0.$$

Proof. This is a direct consequence of **(A3)** with $g = f$ and $g = -1$, respectively. ∎

Next, we consider the convergence of the representation of the Eulerian derivatives. Recall that for $V \in W^{1,\infty}(D)$ we have

$$\begin{aligned} J'(\Omega; V) &= \int_\Omega u\,(\operatorname{div} V) + (\nabla u)^\top \left[(\operatorname{div} V)\,\mathrm{id} - DV - DV^\top\right] \nabla p - \operatorname{div}(f\,V)\,p\,\mathrm{d}x \\ &= \int_\Omega G_0 \cdot V + G_1 : DV \,\mathrm{d}x \end{aligned}$$

with

$$G_0 = -p\,\nabla f, \qquad G_1 = (u + \nabla u \cdot \nabla p - f\,p)\,\mathrm{id} - \nabla u\,(\nabla p)^\top - \nabla p\,(\nabla u)^\top. \tag{9.2}$$

Note that $G_0 = 0$ and $G_1 = 0$ a.e. on $D \setminus \Omega$. Similarly we obtain for the discrete Eulerian derivative

$$\begin{aligned} J_n'(\Omega_n; V_n) &= \int_\Omega u_n\,(\operatorname{div} V_n) + (\nabla u_n)^\top \left[(\operatorname{div} V_n)\,\mathrm{id} - DV_n - DV_n^\top\right] \nabla p_n \,\mathrm{d}x \\ &\qquad - \int_\Omega \operatorname{div}(f\,V_n)\,p_n\,\mathrm{d}x \\ &= \int_\Omega G_{0,n} \cdot V_n + G_{1,n} : DV_n \,\mathrm{d}x \end{aligned}$$

for all $V_n \in S^1(\Omega_n)^d$ with

$$G_{0,n} = -p_n \nabla f, \tag{9.3a}$$

$$G_{1,n} = (u_n + \nabla u_n \cdot \nabla p_n - f\, p_n)\, \mathrm{id} - \nabla u_n\, (\nabla p_n)^\top - \nabla p_n\, (\nabla u_n)^\top. \tag{9.3b}$$

Now, it is clear that Lemma 9.3 implies

$$\|G_0 - G_{0,n}\|_{L^2(D)^d} + \|G_1 - G_{1,n}\|_{L^2(D)^{d\times d}} \to 0.$$

Next, we are going to exploit the stationarity of Ω_n in the sense of (5.16). In particular, we use the characterization (5.17) in terms of the shape gradient $V_{\mathrm{grad},n} \in S^1(\Omega_n)^d$, i.e., the solution $V_{\mathrm{grad},n} \in S^1(\Omega_n)^d$ of

$$\langle E_n V_{\mathrm{grad},n},\, Z_n\rangle = J_n'(\Omega_n; Z_n) = \int_{\Omega_n} G_{0,n} \cdot Z_n + G_{1,n} : DZ_n \,\mathrm{d}x \qquad \forall Z_n \in S^1(\Omega_n)^d$$

satisfies

$$\int_{\partial\Omega_n} (V_{\mathrm{grad},n} \cdot \nu_n)\, \varphi_n \,\mathrm{d}x = 0 \qquad \forall \varphi_n \in S^1(\partial\Omega_n).$$

The next result shows that we can pass to the limit in these two equations.

Lemma 9.4. *We denote by $V_{\mathrm{grad}} \in H^1(\Omega)^d$ the solution of*

$$\langle E\, V_{\mathrm{grad},h},\, Z\rangle = J'(\Omega; Z) = \int_{\Omega} G_0 \cdot Z + G_1 : DZ \,\mathrm{d}x \qquad \forall Z \in H^1(\Omega)^d.$$

Then,

$$\int_{\partial\Omega} (V_{\mathrm{grad}} \cdot \nu)\, \varphi \,\mathrm{d}x = 0 \qquad \forall \varphi \in L^2(\partial\Omega).$$

Proof. We first consider the case of φ being Lipschitz continuous. Then, φ can be extended to a function $\varphi \in W^{1,\infty}(D)$. We denote by $\widetilde{V_{\mathrm{grad},n}} \in S^1(\Omega_n)^d$ the solution of

$$\langle E\, \widetilde{V_{\mathrm{grad},n}},\, Z_n\rangle = \int_{\Omega_n} G_0 \cdot Z_n + G_1 : DZ_n \,\mathrm{d}x \qquad \forall Z_n \in S^1(\Omega_n)^d.$$

The stability of the Galerkin scheme implies

$$\begin{aligned} \|V_{\mathrm{grad},n} - \widetilde{V_{\mathrm{grad},n}}\|_{H^1(\Omega_n)^d} &\le C\left(\|G_0 - G_{0,n}\|_{L^2(\Omega_n)^d} + \|G_1 - G_{1,n}\|_{L^2(\Omega_n)^{d\times d}}\right) \\ &\le C\left(\|G_0 - G_{0,n}\|_{L^2(D)^d} + \|G_1 - G_{1,n}\|_{L^2(D)^{d\times d}}\right) \to 0. \end{aligned}$$

Now, we use the divergence theorem to obtain

$$\begin{aligned} \left|\int_{\partial\Omega_n} (V_{\mathrm{grad},n} - \widetilde{V_{\mathrm{grad},n}}) \cdot \nu_n\, \varphi \,\mathrm{d}s\right| &= \left|\int_{\Omega_n} \operatorname{div}\big((V_{\mathrm{grad},n} - \widetilde{V_{\mathrm{grad},n}})\, \varphi\big) \,\mathrm{d}x\right| \\ &\le C\, \|V_{\mathrm{grad},n} - \widetilde{V_{\mathrm{grad},n}}\|_{H^1(\Omega_n)^d}\, \|\varphi\|_{H^1(\Omega_n)} \to 0. \end{aligned}$$

By definition of $\widetilde{V_{\mathrm{grad},n}}$, we can invoke **(A4)** to obtain

$$\int_{\partial\Omega_n} (\widetilde{V_{\mathrm{grad},n}} \cdot \nu_n)\, \varphi \,\mathrm{d}s \to \int_{\partial\Omega} (V_{\mathrm{grad}} \cdot \nu)\, \varphi \,\mathrm{d}s.$$

Together with the previous estimate, we obtain

$$\int_{\partial\Omega_n} (V_{\mathrm{grad},n} \cdot \nu_n)\, \varphi \, \mathrm{d}s \to \int_{\partial\Omega} (V_{\mathrm{grad}} \cdot \nu)\, \varphi \, \mathrm{d}s.$$

Thus, it remains to prove

$$\int_{\partial\Omega_n} (V_{\mathrm{grad},n} \cdot \nu_n)\, \varphi \, \mathrm{d}s \to 0.$$

Since φ is Lipschitz continuous, **(A2)** implies the existence of $\varphi_n \in S^1(\partial\Omega_n)$ such that

$$\|\varphi - \varphi_n\|_{L^\infty(\partial\Omega_n)} \le C\, \|\varphi - \varphi_n\|_{L^\infty(\Omega_n)} \le C\, h_n\, \|\varphi\|_{W^{1,\infty}(D)}.$$

Together with the stationarity of Ω_n, we obtain

$$\begin{aligned}\Big|\int_{\partial\Omega_n} (V_{\mathrm{grad},n} \cdot \nu_n)\, \varphi \, \mathrm{d}s\Big| &= \Big|\int_{\partial\Omega_n} (V_{\mathrm{grad},n} \cdot \nu_n)\, (\varphi - \varphi_n) \, \mathrm{d}s\Big| \\ &\le C\, \|V_{\mathrm{grad},n}\|_{L^1(\partial\Omega_n)^d}\, \|\varphi - \varphi_n\|_{L^\infty(\partial\Omega_n)} \\ &\le C\, \|V_{\mathrm{grad},n}\|_{H^1(\Omega_n)^d}\, \|\varphi - \varphi_n\|_{L^\infty(\partial\Omega_n)} \to 0.\end{aligned}$$

Note that we have used **(A5)** in the final inequality. This shows the claim in the case that φ is Lipschitz. Finally, the density of Lipschitz functions in $L^2(\partial\Omega)$ and $V_{\mathrm{grad}} \cdot \nu \in L^2(\partial\Omega)$ implies the claim. ∎

With the above preparations, we can prove our main theorem.

THEOREM 9.5. *The limit domain Ω is stationary, i.e., $J'(\Omega;\cdot) = 0$ holds.*

Proof. Since Ω is assumed to have a $C^{1,1}$ boundary, we obtain from Corollary 3.2 that

$$J'(\Omega; V) = \int_{\partial\Omega} g_\Omega\, (V \cdot \nu)\, \mathrm{d}s$$

holds with

$$g_\Omega = -\frac{\partial u}{\partial \nu}\, \frac{\partial p}{\partial \nu} \in L^2(\partial\Omega).$$

Now, using $Z = V_{\mathrm{grad}}$ in the equation for V_{grad}, we obtain

$$\langle E V_{\mathrm{grad}},\, V_{\mathrm{grad}}\rangle = J'(\Omega; V_{\mathrm{grad}}) = \int_{\partial\Omega} g_\Omega\, (V_{\mathrm{grad}} \cdot \nu)\, \mathrm{d}s.$$

Lemma 9.4 implies

$$\langle E V_{\mathrm{grad}},\, V_{\mathrm{grad}}\rangle = 0.$$

Hence, $V_{\mathrm{grad}} = 0$ and, thus, $J'(\Omega;\cdot) = 0$. ∎

10. Conclusions. In this paper we introduce the concept of restricted mesh deformations for the computational solution of shape optimization problems involving PDEs. In a nutshell, we only admit perturbations fields which are induced by normal boundary forces. We argue that the stationarity condition (5.11) which does not impose any restriction on the mesh deformations leads to degenerate meshes and premature stopping. By contrast, we were able to solve the corresponding restricted stationarity condition (5.16) to high accuracy even with a gradient method. We also propose a Newton-like method based on restricted mesh deformations which exhibits fast convergence.

Even though we require only the restricted stationarity condition (5.16) to hold, we were able to show in section 9 the convergence of the corresponding discrete shapes towards a stationary point of the continuous problem.

It is not clear whether (5.16) are the optimality conditions of a discrete optimization problem in Euclidean space. We conjecture that (5.16) are the optimality conditions for a problem defined on a discrete shape manifold, whose tangent space is represented by restricted mesh deformations.

References.

Adams, R.; Fournier, J. (2003). *Sobolev Spaces*. 2nd ed. New York: Academic Press.

Attouch, H.; Buttazzo, G.; Michaille, G. (2014). *Variational analysis in Sobolev and BV spaces*. 2nd ed. Vol. 17. MOS-SIAM Series on Optimization. Applications to PDEs and optimization. Society for Industrial and Applied Mathematics (SIAM), Philadelphia, PA; Mathematical Optimization Society, Philadelphia, PA, pp. xii+793. DOI: 10.1137/1.9781611973488.

Bänsch, E.; Morin, P.; Nochetto, R. H. (2005). "A finite element method for surface diffusion: the parametric case". *Journal of Computational Physics* 203.1, pp. 321–343. DOI: 10.1016/j.jcp.2004.08.022.

Berggren, M. (2010). "A unified discrete-continuous sensitivity analysis method for shape optimization". *Applied and numerical partial differential equations*. Vol. 15. Computational Methods in Applied Sciences. Springer, New York, pp. 25–39. DOI: 10.1007/978-90-481-3239-3_4.

Bonito, A.; Nochetto, R. H.; Pauletti, M. S. (2010). "Geometrically consistent mesh modification". *SIAM Journal on Numerical Analysis* 48.5, pp. 1877–1899. DOI: 10.1137/100781833.

Delfour, M.; Payre, G.; Zolesio, J.-P. (1985). "An optimal triangulation for second-order elliptic problems". *Computer Methods in Applied Mechanics and Engineering* 50, pp. 231–261. DOI: 10.1016/0045-7825(85)90095-7.

Delfour, M.; Zolésio, J.-P. (2011). *Shapes and Geometries*. 2nd ed. Society for Industrial and Applied Mathematics. DOI: 10.1137/1.9780898719826.

Doğan, G.; Morin, P.; Nochetto, R. H.; Verani, M. (2007). "Discrete gradient flows for shape optimization and applications". *Computer Methods in Applied Mechanics and Engineering* 196.37-40, pp. 3898–3914. DOI: 10.1016/j.cma.2006.10.046.

Dokken, J. S.; Funke, S. W.; Johansson, A.; Schmidt, S. (2018). *Shape Optimization using the Finite Element Method on Multiple Meshes*. arXiv: 1806.09821.

Eppler, K.; Harbrecht, H. (2005). "A regularized Newton method in electrical impedance tomography using shape Hessian information". *Control and Cybernetics* 34.1, pp. 203–225.

Eppler, K.; Harbrecht, H.; Schneider, R. (2007). "On convergence in elliptic shape optimization". *SIAM Journal on Control and Optimization* 46.1, pp. 61–83. DOI: 10.1137/05062679X.

Feppon, F.; Allaire, G.; Bordeu, F.; Cortial, J.; Dapogny, C. (2018). *Shape Optimization of a Coupled Thermal Fluid-Structure Problem in a Level Set Mesh Evolution Framework*. HAL: hal-01686770.

Fumagalli, I.; Parolini, N.; Verani, M. (2015). “Shape optimization for Stokes flows: a finite element convergence analysis”. *European Series in Applied and Industrial Mathematics (ESAIM): Mathematical Modelling and Numerical Analysis* 49.4, pp. 921–951. DOI: 10.1051/m2an/2014060.

Gangl, P.; Langer, U.; Laurain, A.; Meftahi, H.; Sturm, K. (2015). *Shape Optimization of an Electric Motor subject to Nonlinear Magnetostatics*. Tech. rep. eprint: arXiv: 1501.04752.

Giacomini, M.; Pantz, O.; Trabelsi, K. (2017). “Certified descent algorithm for shape optimization driven by fully-computable *a posteriori* error estimators”. *ESAIM. Control, Optimisation and Calculus of Variations* 23.3, pp. 977–1001. DOI: 10.1051/cocv/2016021.

Haslinger, J.; Mäkinen, R. (2003). *Introduction to Shape Optimization*. Philadelphia: SIAM.

Hiptmair, R.; Paganini, A.; Sargheini, S. (2015). “Comparison of approximate shape gradients”. *BIT. Numerical Mathematics* 55.2, pp. 459–485. DOI: 10.1007/s10543-014-0515-z.

Iglesias, J. A.; Sturm, K.; Wechsung, F. (2017). *Shape optimisation with nearly conformal transformations*. Tech. rep. eprint: arXiv:1710.06496.

Ito, K.; Kunisch, K.; Peichl, G. H. (2008). “Variational approach to shape derivatives”. *ESAIM. Control, Optimisation and Calculus of Variations* 14.3, pp. 517–539. DOI: 10.1051/cocv:2008002.

Kiniger, B.; Vexler, B. (2013). “*A priori* error estimates for finite element discretizations of a shape optimization problem”. *European Series in Applied and Industrial Mathematics (ESAIM): Mathematical Modelling and Numerical Analysis* 47.6, pp. 1733–1763. DOI: 10.1051/m2an/2013086.

Laurain, A.; Sturm, K. (2016). “Distributed shape derivative via averaged adjoint method and applications”. *ESAIM. Mathematical Modelling and Numerical Analysis* 50.4, pp. 1241–1267. DOI: 10.1051/m2an/2015075.

Li, X. S. (2005). “An overview of SuperLU: algorithms, implementation, and user interface”. *Association for Computing Machinery. Transactions on Mathematical Software* 31.3, pp. 302–325. DOI: 10.1145/1089014.1089017.

Logg, A.; Mardal, K.-A.; Wells, G. N., et al. (2012). *Automated Solution of Differential Equations by the Finite Element Method*. Springer. DOI: 10.1007/978-3-642-23099-8.

Luenberger, D. G. (1969). *Optimization by Vector Space Methods*. John Wiley.

Mignot, F. (1976). “Contrôle dans les inéquations variationelles elliptiques”. *Journal of Functional Analysis* 22.2, pp. 130–185.

Morin, P.; Nochetto, R. H.; Pauletti, M. S.; Verani, M. (2012). “Adaptive finite element method for shape optimization”. *ESAIM. Control, Optimisation and Calculus of Variations* 18.4, pp. 1122–1149. DOI: 10.1051/cocv/2011192.

Novruzi, A.; Roche, J. R. (2000). “Newton’s method in shape optimisation: a three-dimensional case”. *BIT. Numerical Mathematics* 40.1, pp. 102–120. DOI: 10.1023/A:1022370419231.

Roth, R.; Ulbrich, S. (Jan. 2013). “A Discrete Adjoint Approach for the Optimization of Unsteady Turbulent Flows”. *Flow, Turbulence and Combustion* 90.4, pp. 763–783. DOI: 10.1007/s10494-012-9439-3.

Schmidt, S.; Gauger, N.; Ilic, C.; Schulz, V. (June 2011). “Three Dimensional Large Scale Aerodynamic Shape Optimization based on Shape Calculus”. *41st AIAA Fluid Dynamics Conference and Exhibit*. American Institute of Aeronautics and Astronautics. DOI: 10.2514/6.2011-3718.

Schmidt, S.; Schulz, V. H. (2009). "Impulse response approximations of discrete shape Hessians with application in CFD". *SIAM Journal on Control and Optimization* 48.4, pp. 2562–2580. DOI: 10.1137/080719844.

Schmidt, S.; Schulz, V. H. (2010). "Shape derivatives for general objective functions and the incompressible Navier-Stokes equations". *Control and Cybernetics* 39.3, pp. 677–713.

Schneider, R.; Jimack, P. K. (2008). "On the evaluation of finite element sensitivities to nodal coordinates". *Electronic Transactions on Numerical Analysis* 32, pp. 134–144.

Schulz, V. H. (2014). "A Riemannian view on shape optimization". *Foundations of Computational Mathematics. The Journal of the Society for the Foundations of Computational Mathematics* 14.3, pp. 483–501. DOI: 10.1007/s10208-014-9200-5.

Schulz, V. H.; Siebenborn, M. (2016). "Computational comparison of surface metrics for PDE constrained shape optimization". *Computational Methods in Applied Mathematics* 16.3, pp. 485–496. DOI: 10.1515/cmam-2016-0009.

Schulz, V. H.; Siebenborn, M.; Welker, K. (2015). "Structured inverse modeling in parabolic diffusion problems". *SIAM Journal on Control and Optimization* 53.6, pp. 3319–3338. DOI: 10.1137/140985883.

Schulz, V. H.; Siebenborn, M.; Welker, K. (2016). "Efficient PDE constrained shape optimization based on Steklov-Poincaré type metrics". *SIAM Journal on Optimization* 26.4, pp. 2800–2819. DOI: 10.1137/15M1029369.

Sokołowski, J.; Zolésio, J.-P. (1992). *Introduction to Shape Optimization*. New York: Springer.

Sturm, K. (2015). "Minimax Lagrangian Approach to the Differentiability of Nonlinear PDE Constrained Shape Functions without Saddle Point Assumptions". *SIAM Journal on Control and Optimization* 53.4, pp. 2017–2039. DOI: 10.1137/130930807.

Sturm, K. (2016). "Shape optimization with nonsmooth cost functions: from theory to numerics". *SIAM Journal on Control and Optimization* 54.6, pp. 3319–3346. DOI: 10.1137/16M1069882.

Udawalpola, R.; Berggren, M. (2008). "Optimization of an acoustic horn with respect to efficiency and directivity". *International Journal for Numerical Methods in Engineering* 73.11, pp. 1571–1606. DOI: 10.1002/nme.2132.

Wachsmuth, G. (2016). "Towards M-stationarity for optimal control of the obstacle problem with control constraints". *SIAM Journal on Control and Optimization* 54.2, pp. 964–986. DOI: 10.1137/140980582.

Wilke, D. N.; Kok, S.; Groenwold, A. A. (2005). "A quadratically convergent unstructured remeshing strategy for shape optimization". *International Journal for Numerical Methods in Engineering* 65.1, pp. 1–17. DOI: 10.1002/nme.1430.

Zunino, P. (June 2004). "Multidimensional Pharmacokinetic Models Applied to the Design of Drug-Eluting Stents". *Cardiovascular Engineering* 4.2, pp. 181–191. DOI: 10.1023/b:care.0000031547.39178.cb.